Crystal Growth of Ternary Compound Semiconductors in Low Gravity Environment

Ching-Hua Su

NASA/Marshall Space Flight Center

Crystal Growth of Ternary Compound Semiconductors

A low gravity material science experiment has been prepared to be performed in the Low Gradient Furnace (LGF) in the Material Science Research Rack (MSRR) on International Space Station (ISS).

There are two sections of the flight experiment:

(I) Investigation toward crystal growth by physical vapor transport (PVT): the growth of ZnSe and related ternary compounds, such as ZnSeS, ZnCdSe, and ZnSeTe,

(II) Investigation on the melt growth of CdTe and CdZnTe by directional solidification.

Crystal Growth Activities at NASA/MSFC

Technological significance:
Growth (melt and vapor) and characterization of II-VI and IV-VI compounds semiconducting materials, such as HgCdTe, HgZnTe (for IR detectors), CdS and ZnO (for UV detector), ZnSe, ZnSeTe (for green /blue laser), CdTe and CdZnTe (for x-ray, gamma ray detectors), PbTe, PbTeSe, and PbSnTe (thermoelectrics).

II	IV	VI
Zn	Sn	O
Cd	Pb	S
Hg		Se
		Te

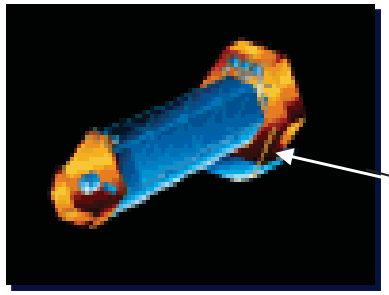

X and gamma ray telescope

CdZnTe FPA

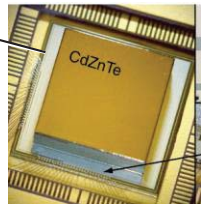

Contributors:

MSFC personnel:
Dr. Sharon Cobb
Dr. Donald Gillies
Dr. Sandor Lehoczky
Dr. Ching-Hua Su
Dr. Martin Volz
Dr. Dale Watring
Dr. Frank Szofran

On-site contractors:
Dr. Shari Feth
Dr. Chao Li
Dr. Konstantine Mazuruk
Dr. N. Ramachandran
Dr. Witold Palosz
Dr. Yigao Sha
Dr. Shen Zhu

II-VI semiconducting compounds grown at MSFC

Compounds	HgTe	HgCdTe	CdTe	CdZnTe	ZnTe	CdS	ZnSe	ZnS
Melting points (°C)	670	700	1092	1130	1292	1397	1526	1718
Melt growth	←	—	—	—	→			
PVT growth temperature (°C)			850		1000	985	1120	1150

Scientific Objectives

1. To establish the relative contributions of gravity-driven fluid flows, both in liquid and vapor, to (1) the non-uniform incorporation of impurities and defects and (2) the deviation from stoichiometry and (3) the compositional variation observed in the grown crystals.

2. To assess the self-induced strain developed during processing at elevated temperatures and retained on cooling caused by the weight of the crystals.

3. The relation between fluid phase processes and the generation of defects in a grown crystal is an outstanding problem in materials growth. Studies in microgravity will be compared with modeling and will lead to a greater understanding of the processes involved.

Phase Diagram of Zn-Se

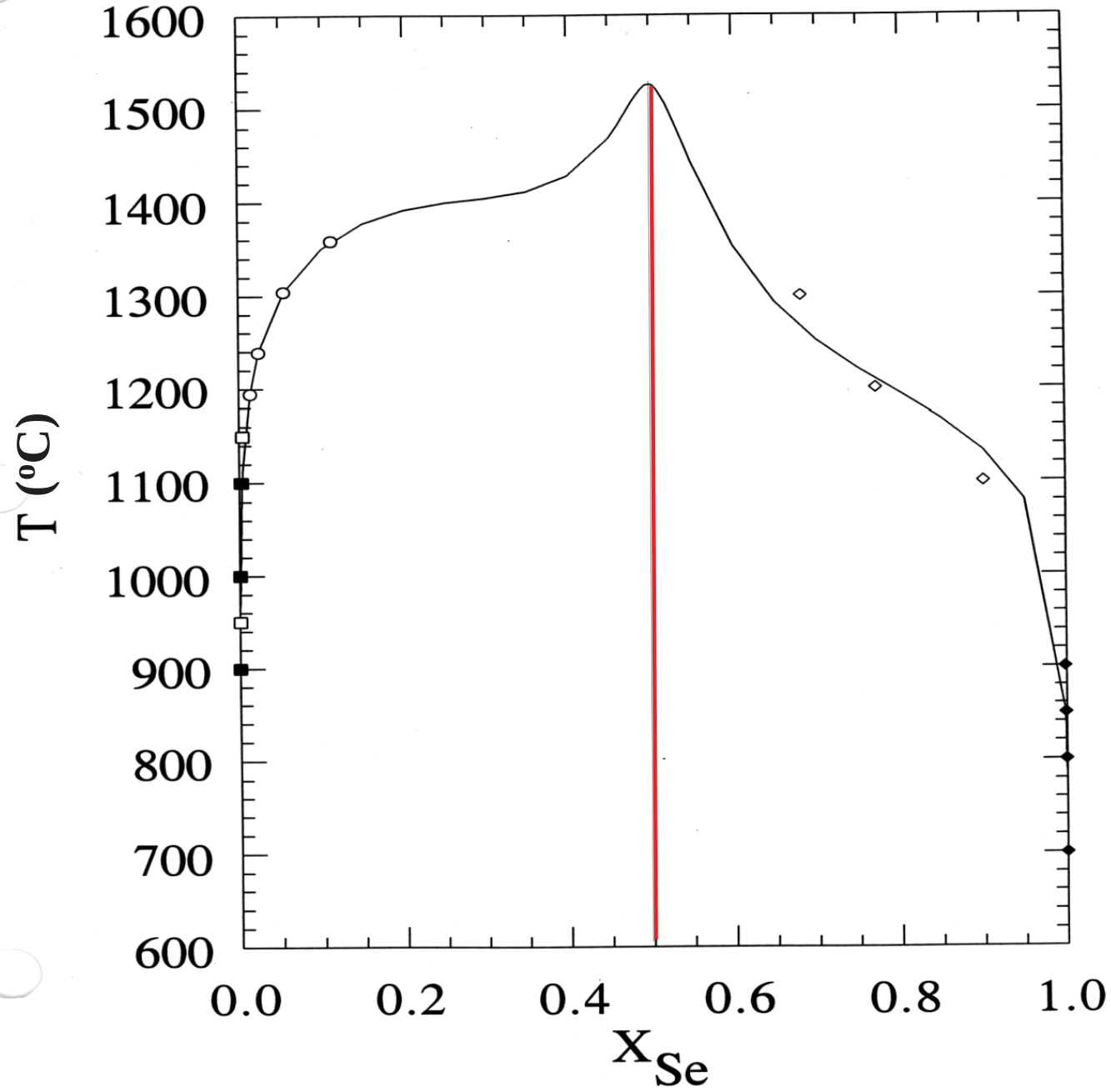

Partial pressures along the three-phase curve for ZnSe(s)

At 1156 °C, P_{Zn} varies from 8.4 to 1.3×10^{-4} atm, P_{Se_2} varies from 20 to 5×10^{-9} atm and $\alpha = P_{Zn} / P_{Se_2}$ varies from 1.7×10^{9} to 6.5×10^{-6}

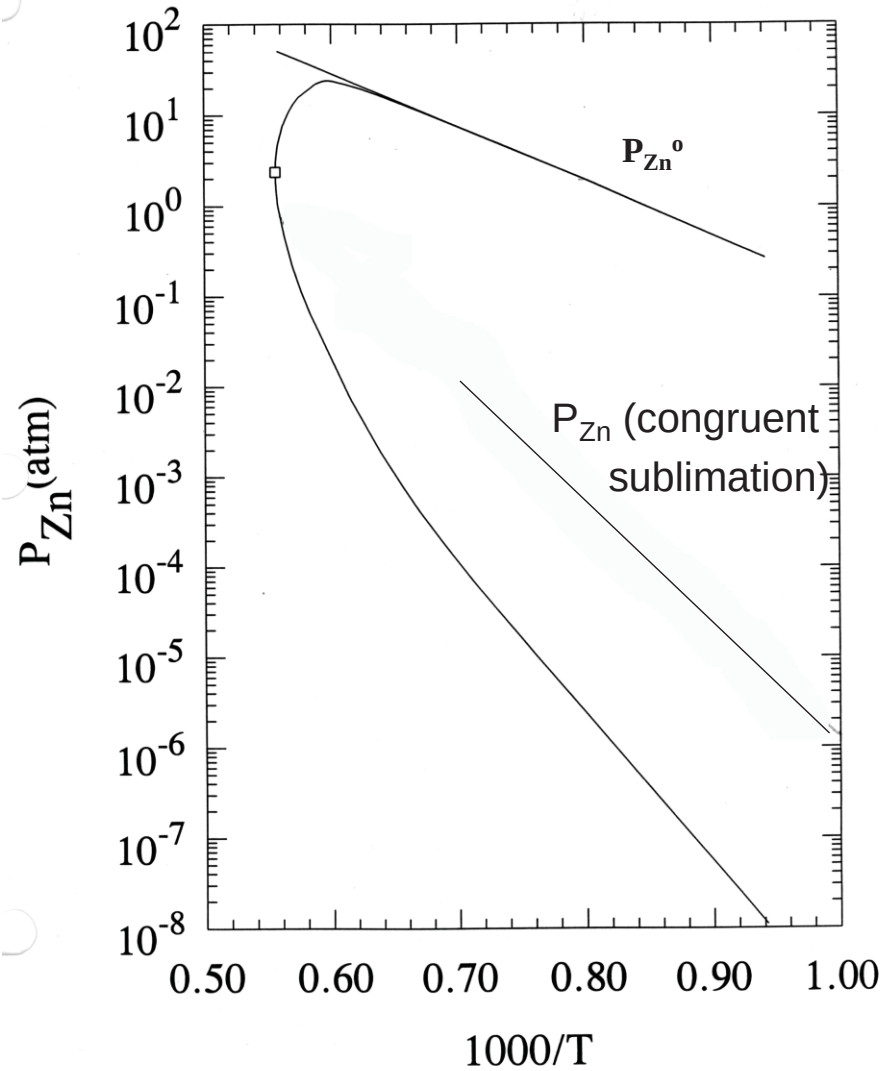

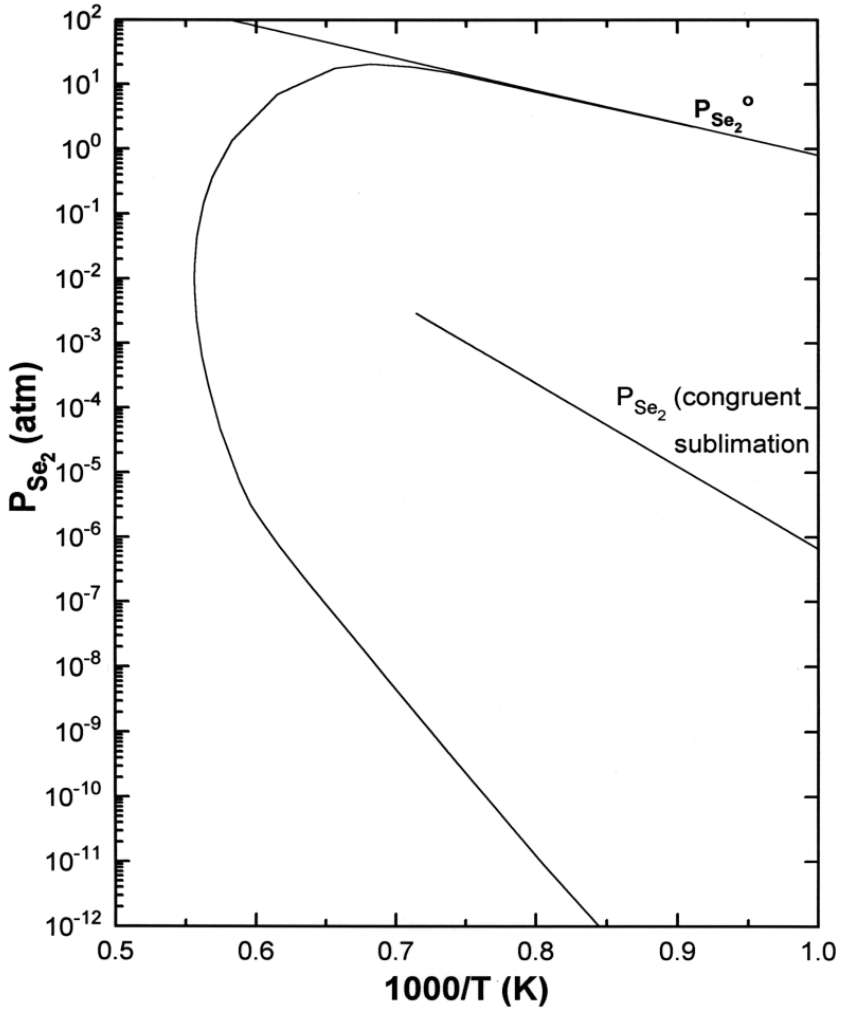

One-Dimensional Diffusion model of PVT

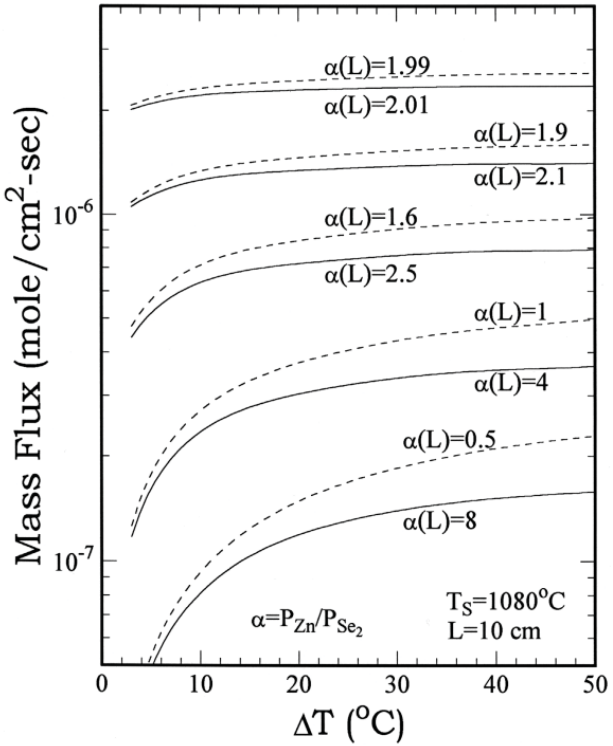

Calculated mass flux of ZnSe as a function of ΔT and different values of α(L). The source temperature was 1080 ℃. Solid lines are for α(L) > 2 and dashed lines are for α(L) < 2.

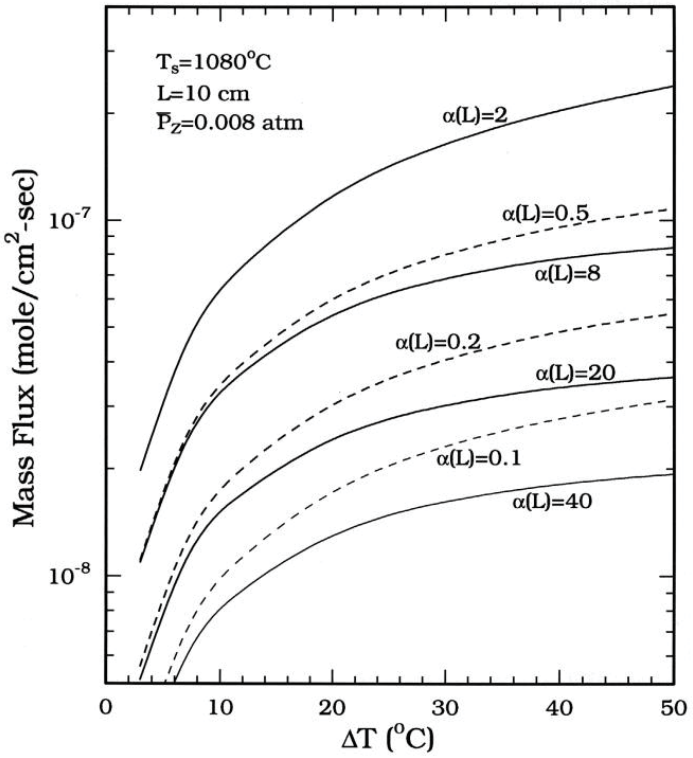

Calculated mass flux of ZnSe as a function of ΔT under the same conditions except a residual gas pressure of 0.008 atm is present in the system.

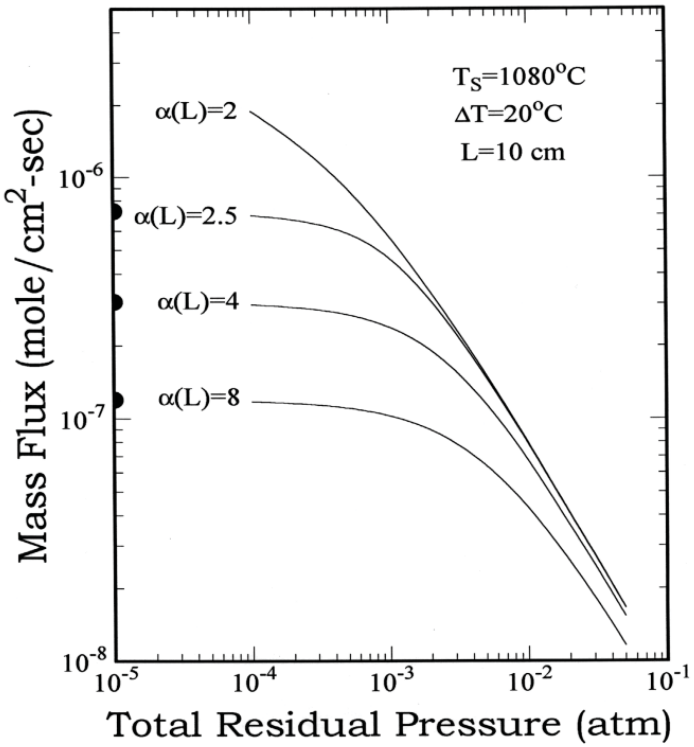

Calculated mass flux of ZnSe as a function of residual gas pressure for source temperature at 1080 ℃ and different values of α(L).

Su, et al. (1998); Sha et al. (1995)

Simultaneous measurements of mass flux and partial pressure

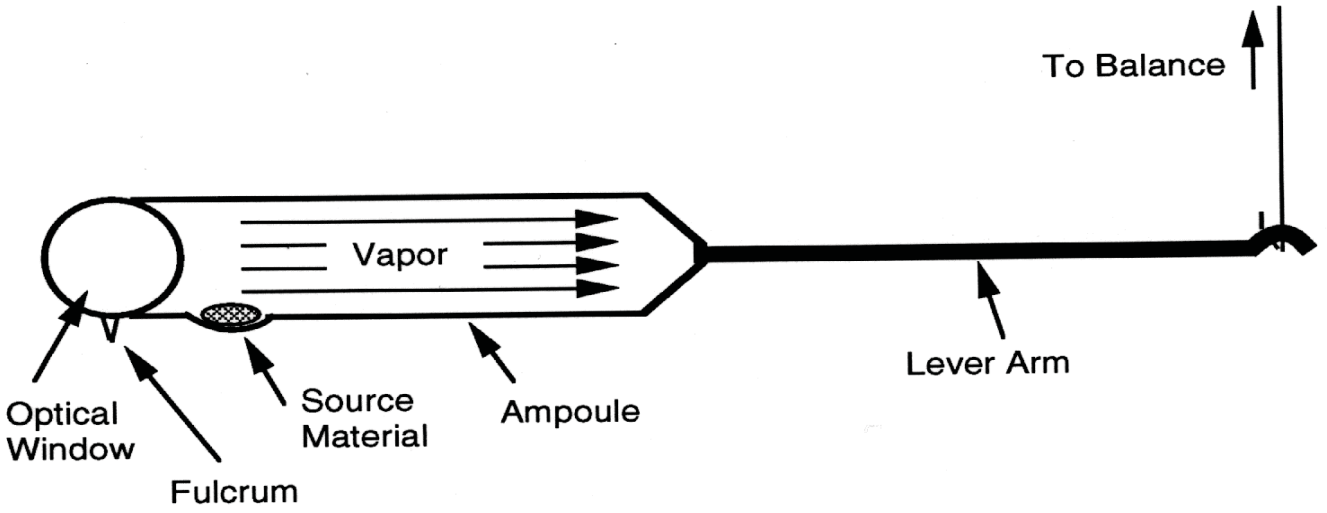

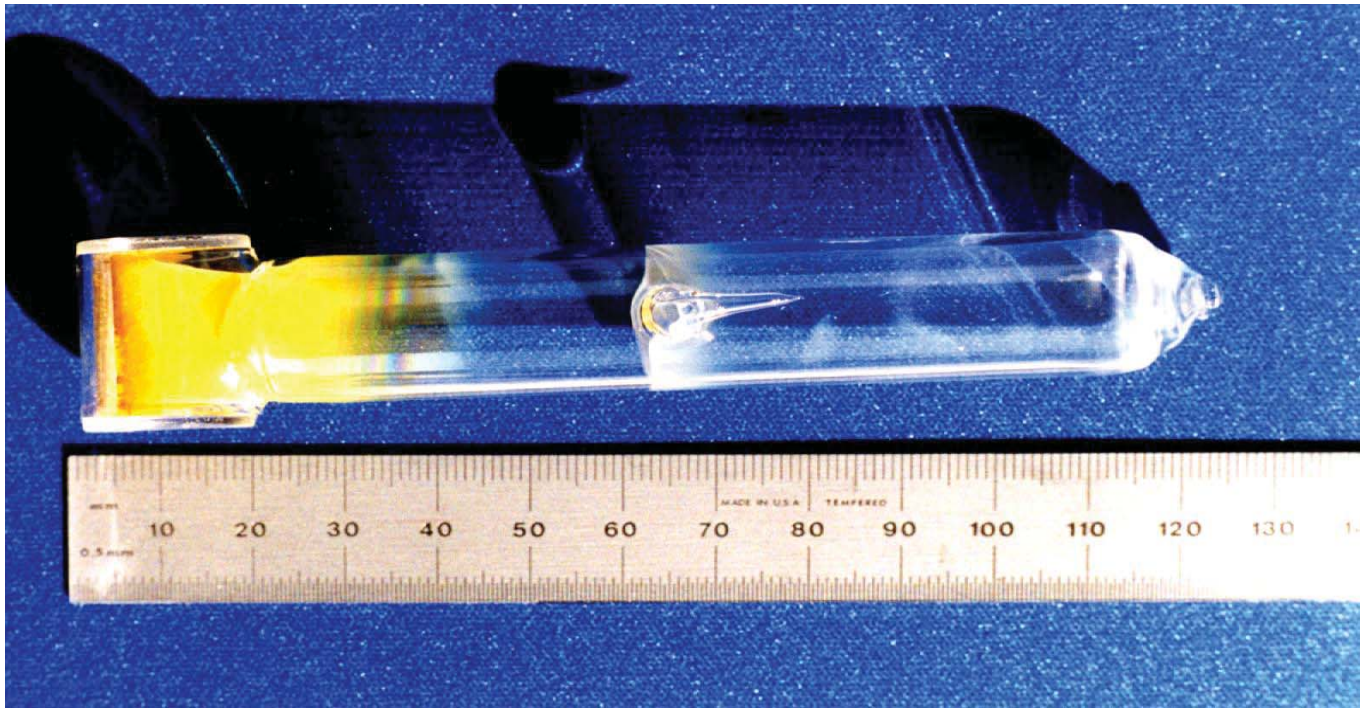

Simultaneous measurements of mass flux and partial pressure

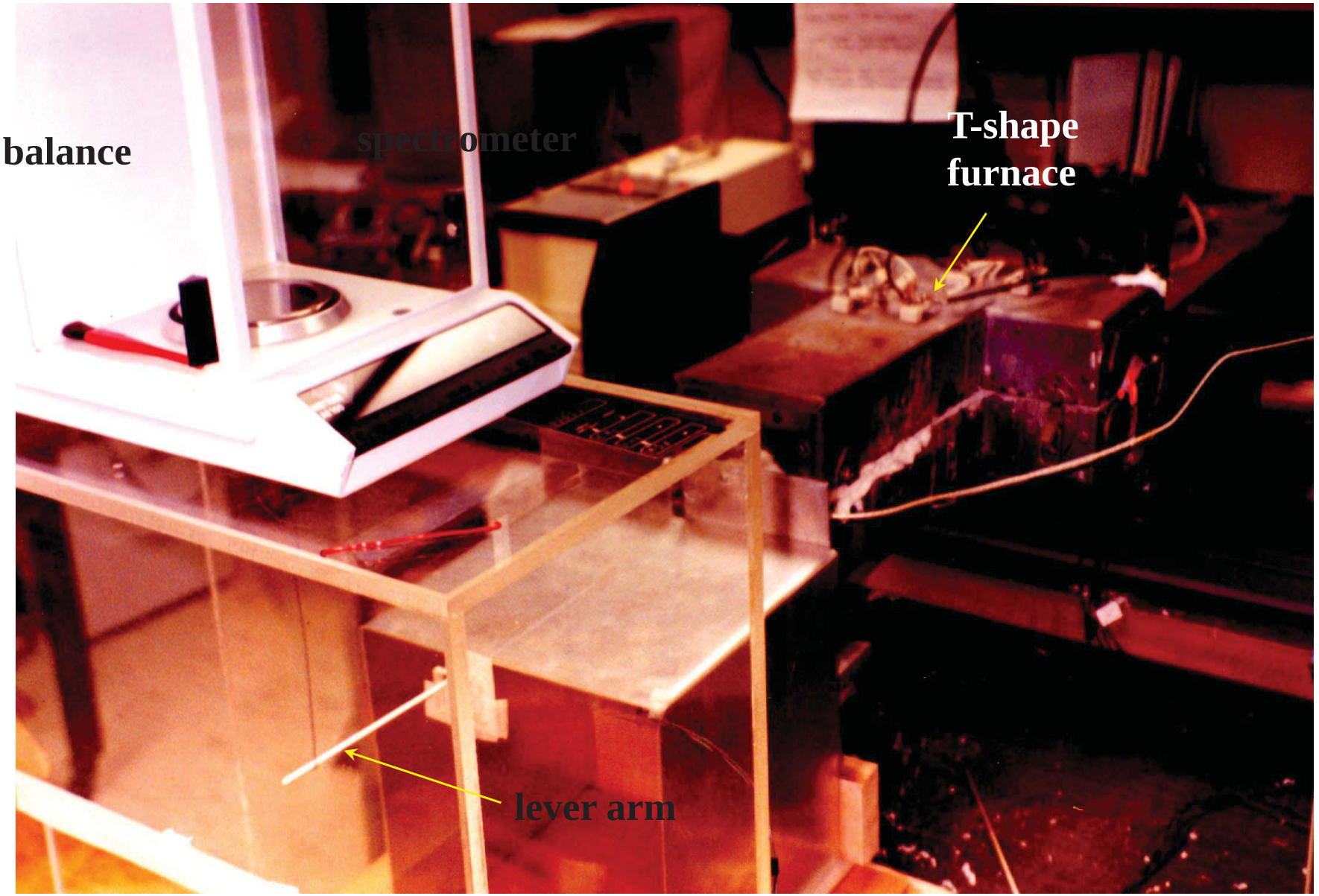

Simultaneous measurements of mass flux and partial pressure

- **P_{Zn} measured over the deposit; α (deposit) = 17.**
- **The measured P_Z value was used in the calculation.**

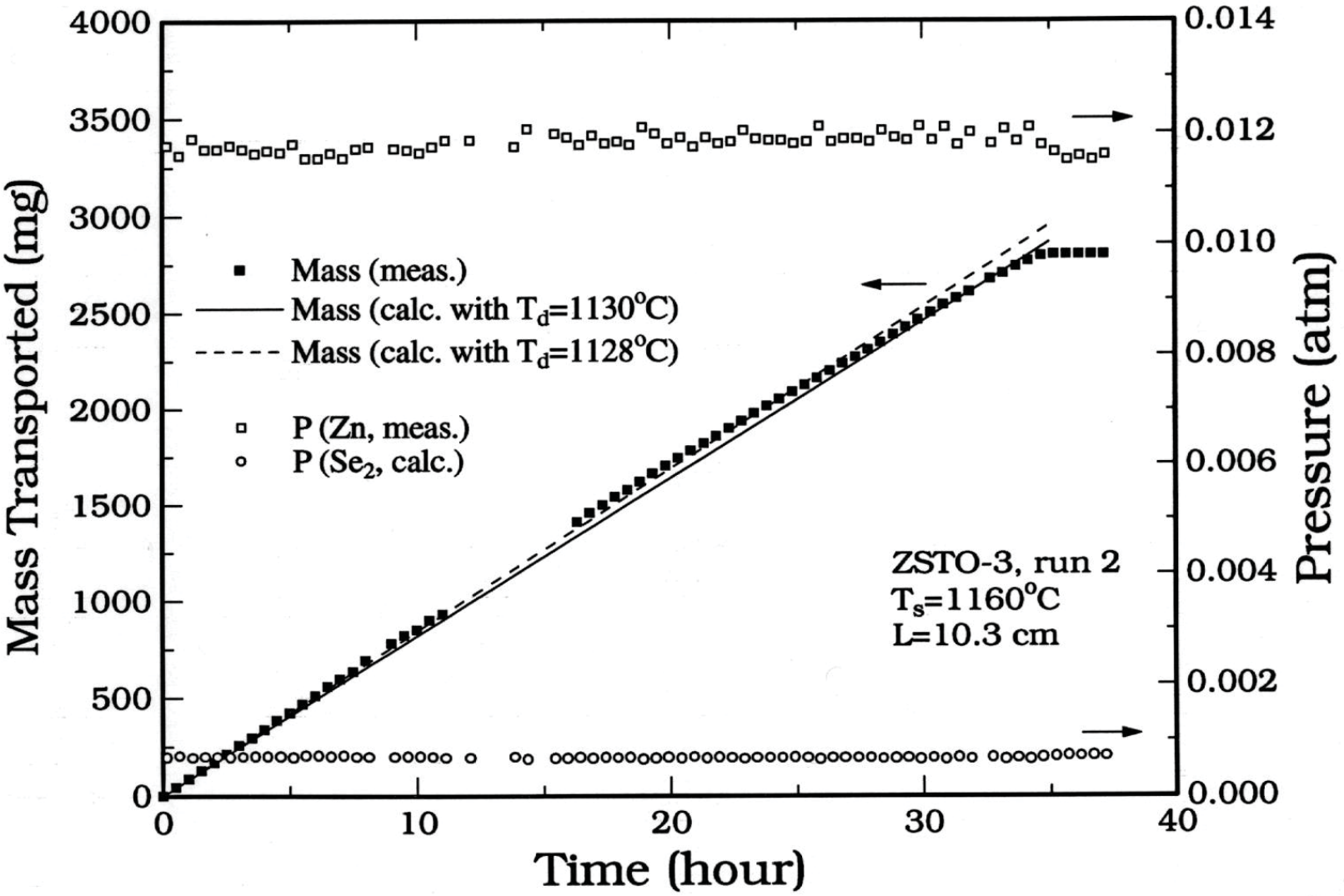

Calculated partial pressure profiles for ZSTO-3 run 2

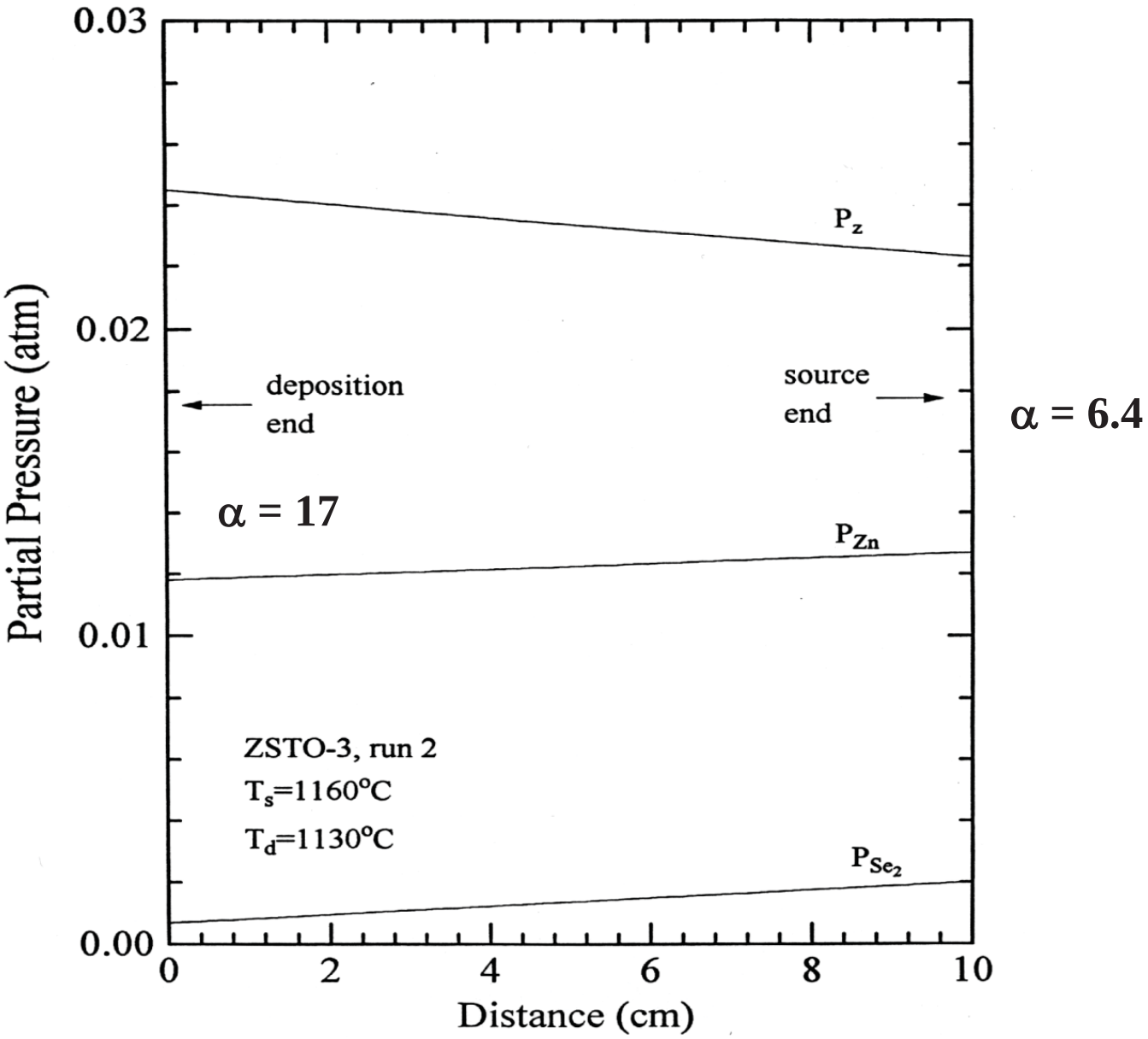

Summary of one dimensional diffusion analysis

- Four experimentally adjustable parameters, the source temperature, the deposition temperature, the partial pressure ratio over source and the residual gas pressure, determine the diffusive mass flux of a PVT system.

- However, two of these four parameters, the partial pressure ratio over source and the residual gas pressure, are more critical than the others. As will be shown, these two parameters are critically dependent on the proper heat treatments of the starting materials for optimum mass flux.

Optimum Heat Treatments of Starting Materials

P_{Se_2} in equilibrium with ZnSe for various optical cells

H_2 reduction and vacuum treatments for ZnSe(O)-3 established to be the optimum procedure

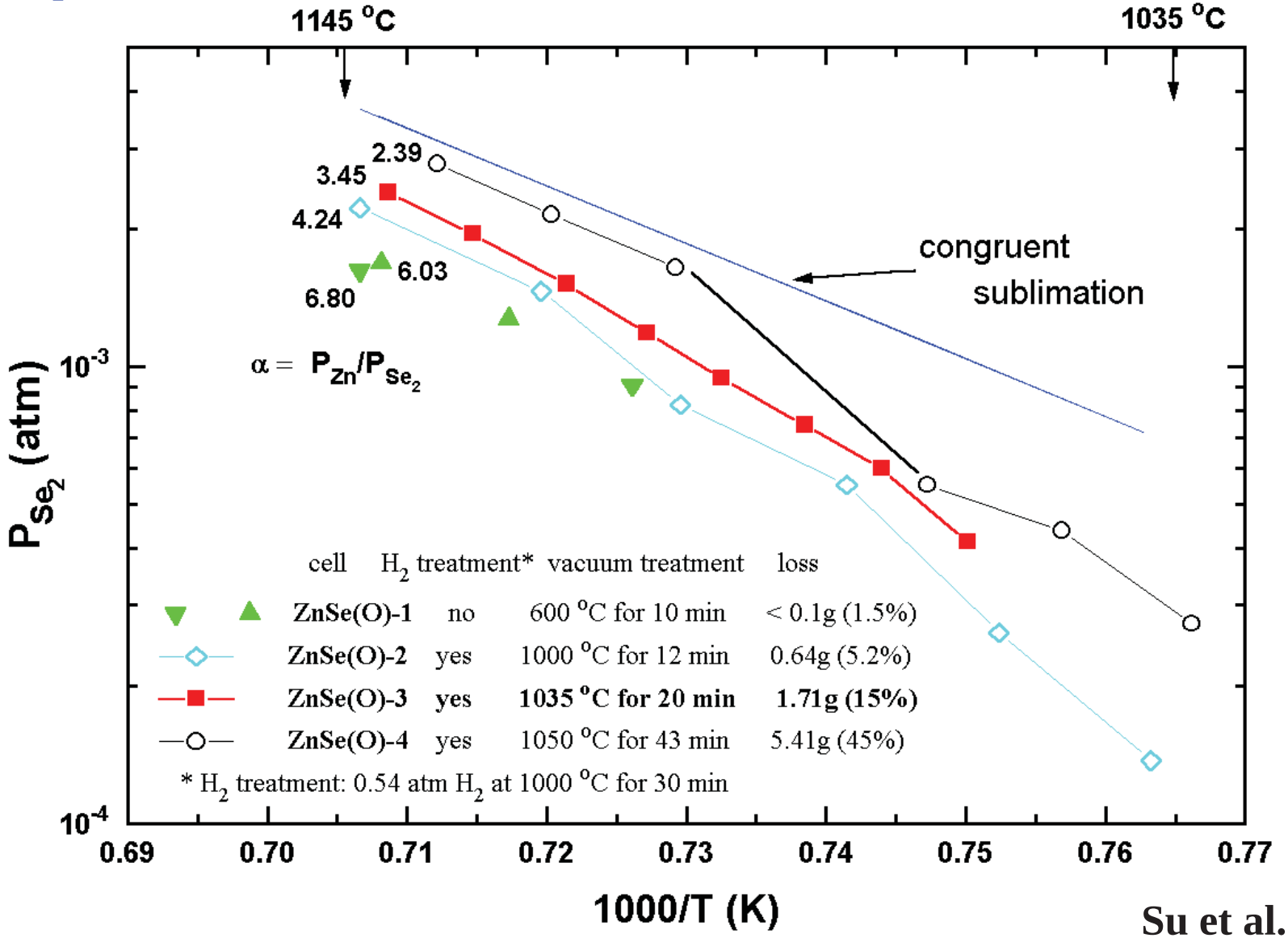

Su et al. (1998)

Crystal Growth by Physical Vapor Transport: temperature profile and initial ampoule positions

- The growth ampoules can be equipped with optical windows to confirm the stoichiometry of the starting material before growth.
- The thermal profile, with a maximum in the middle, was provided by a three-zone furnace with an adiabatic zone between central and cold zones.
- Growth was initiated by translating furnace to the right.

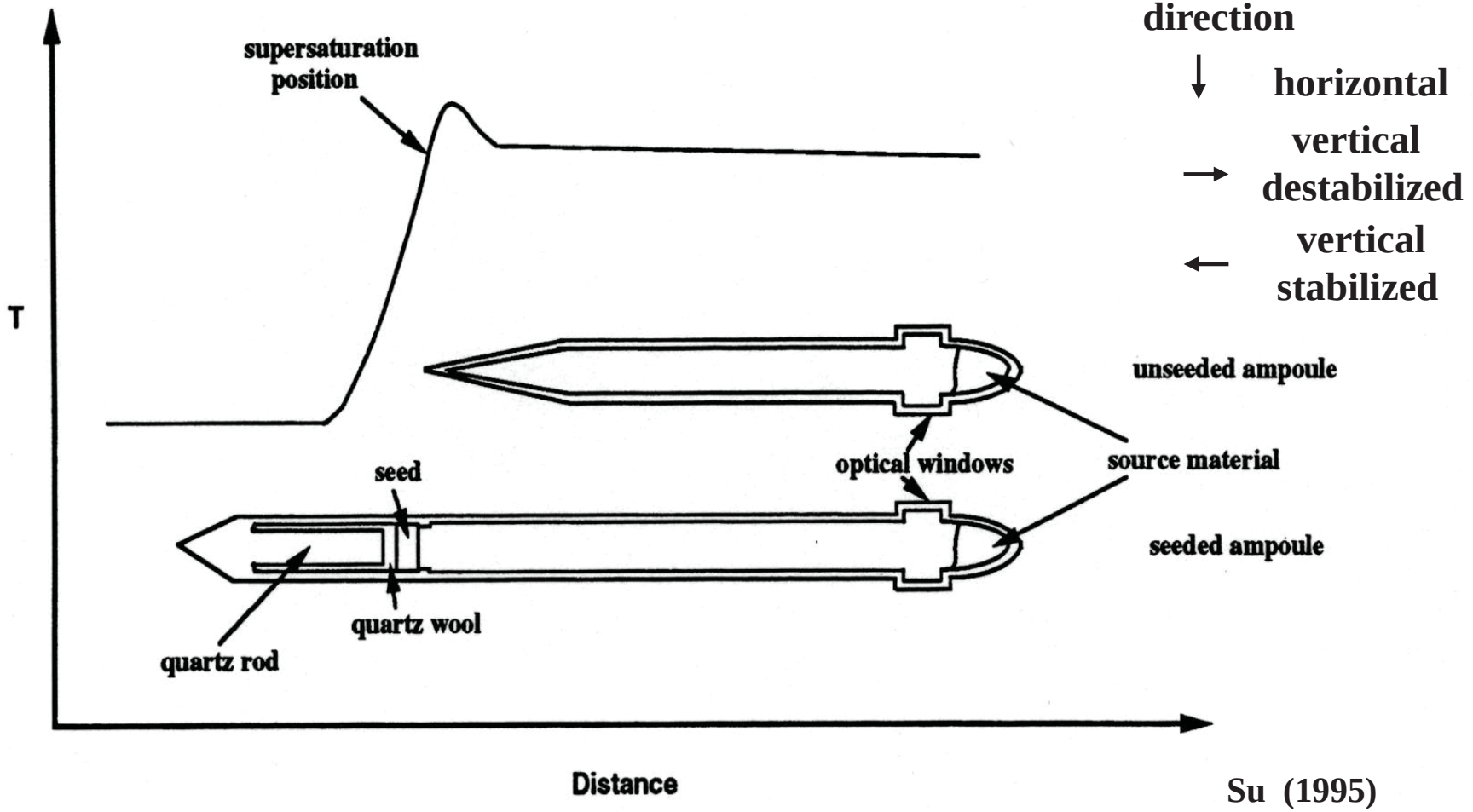

Su (1995)

PVT Growth of ZnSe and Related Ternary Compounds

1. Self-seeded growth of ZnSe in vertical (stabilized and destabilized) and horizontal configurations
2. Seeded growth of ZnSe in vertical and horizontal configurations
3. Self-seeded growth of Cr-doped ZnSe in vertical and horizontal configurations
4. Self-seeded growth of ZnSeTe in vertical and horizontal configurations
5. *In-situ* and real-time optical monitoring of seeded growth in a horizontal configuration

Flow chart of sample characterization plan

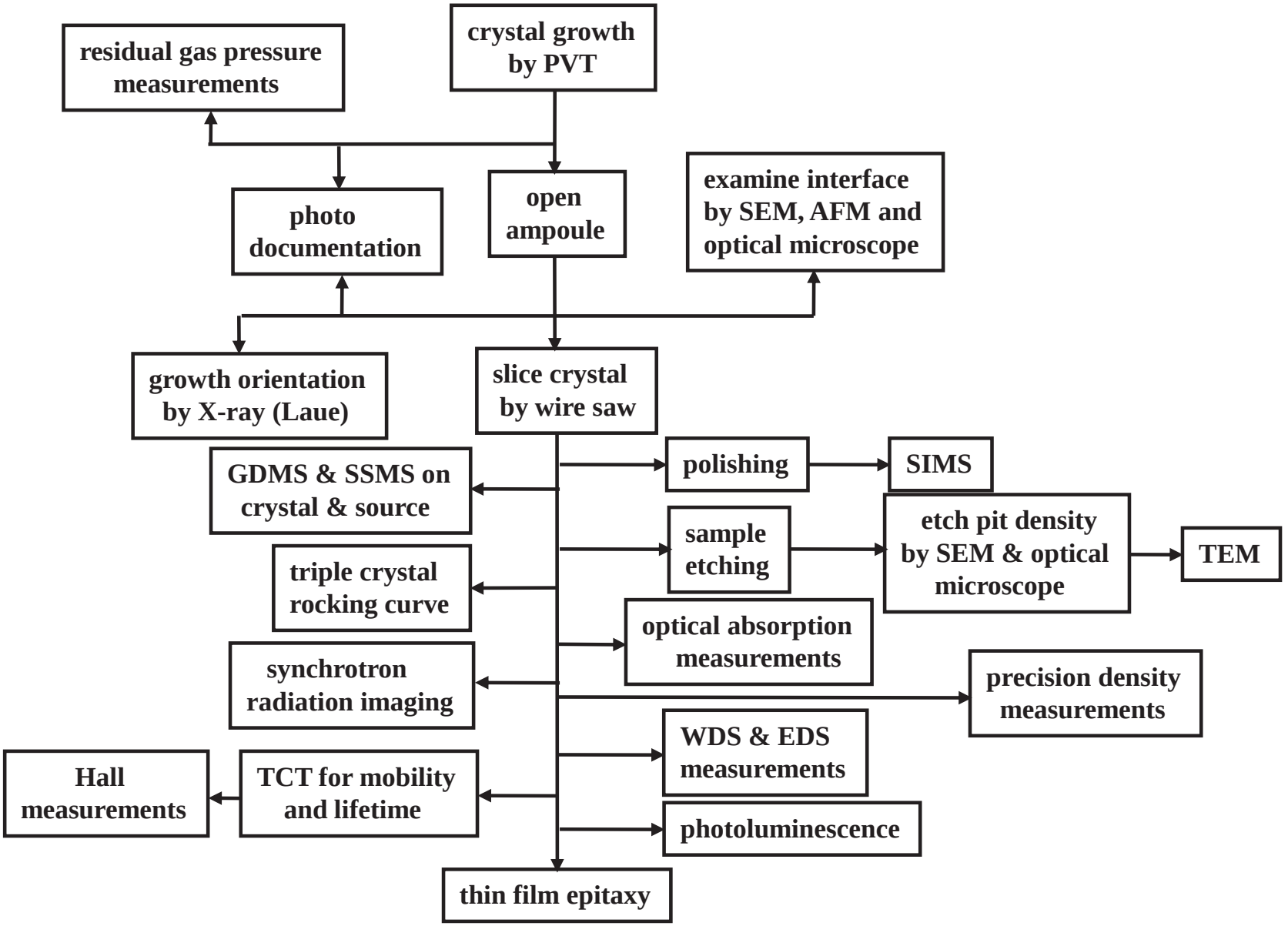

Gravity Effects on the Grown Crystals

Effects were studied by comparing the following characteristics of horizontally and vertically grown ZnSe crystals in :

- Grown crystal morphology : contactless growth for the horizontal configuration.
- Surface morphology of the grown crystals was examined by SEM and AFM. (growth was terminated by stopping furnace translation, lowering the source temperature by 10 ^{o}C and then cooling the thermal profile at the same rate)
- Segregation and distribution of defects and impurities in the grown crystals was determined by photoluminescence, SIMS and precision density measurements.

Gravity Effects on the Grown Crystals

Morphology of the as-grown crystals:

I. Self-seeded ZnSe: Crystals grown in the horizontal configuration grew away from the ampoule wall with large (110) facets tend to align parallel to the gravitational direction. Crystals grown in the vertical configuration grew in contact with the wall to the full diameter.

II. Seeded ZnSe: the as-grown seeded crystals for the horizontal and vertical configurations showed similar characteristics in the morphology as described above for the self-seeded growth.

As-grown surface morphology:

I. As-grown surface of horizontally grown crystals was dominated by (110) terraces and steps (identified to be (221) in one case).

II. As-grown surface of the vertically grown

(a) Crystals showed granular structure with nanotubes (200nm OD, 75nm ID, 25nm in height for one case on ZnSe) on the top.

(b) Some crystals showed a network of high plateau with each island 30 – 70mm in diameter and 3.5mm in height. Numerous nuclei were observed with diameter 20 - 50nm and height of 1 - 7nm on top of these islands.

Morphologies of Self-seeded Vertically Grown ZnSe Crystals

ZnSe-25: vertically stabilized

ZnSe-31: vertically destabilized

ampoule ID: 15mm

g_x

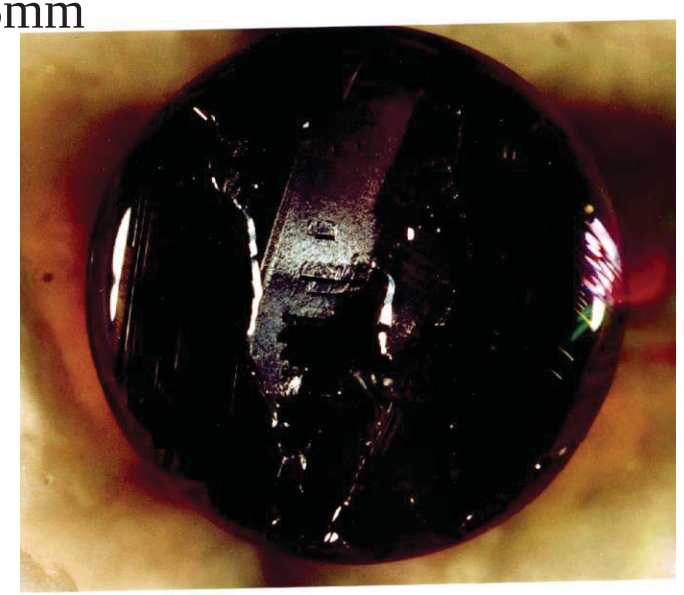

$g_\circ$

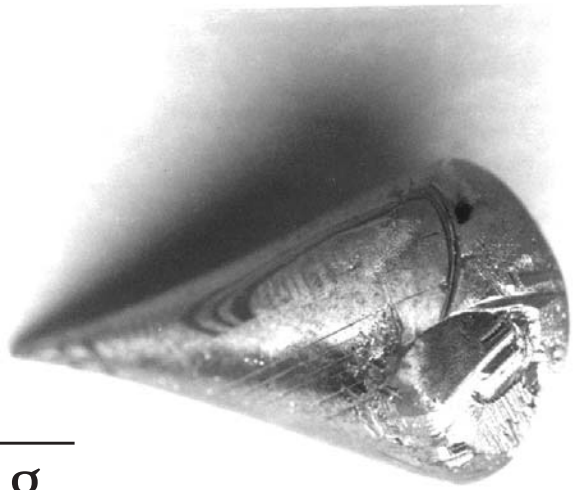

g

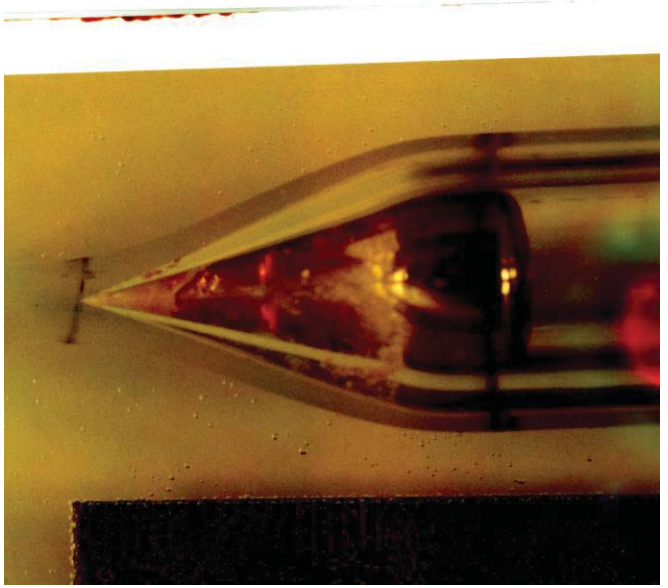

g

Morphologies of Self-seeded Horizontally Grown ZnSe Crystals

ZnSe-44

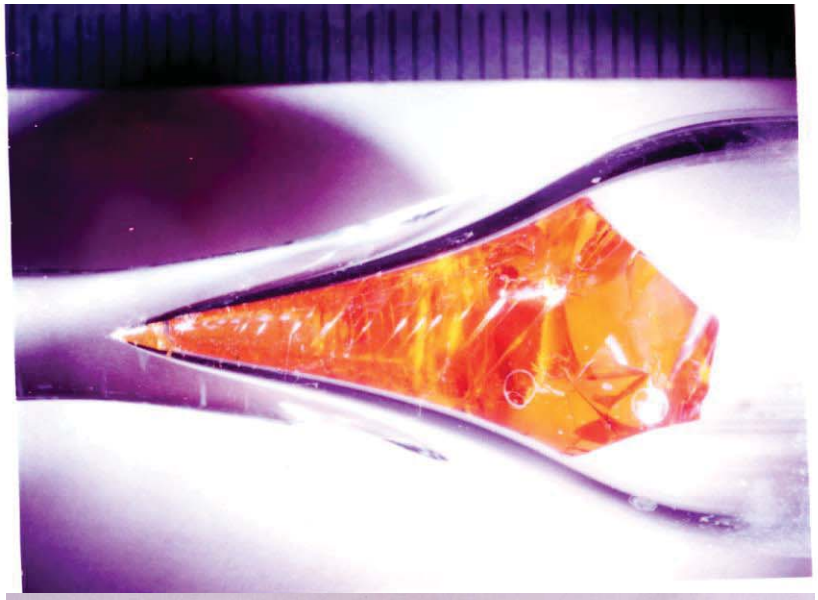

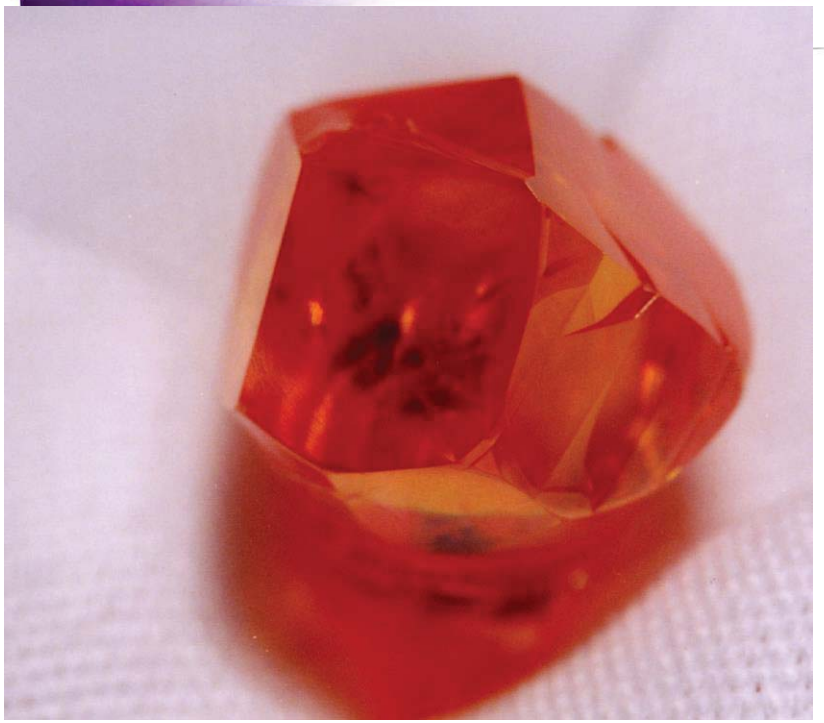

ZnSe-43

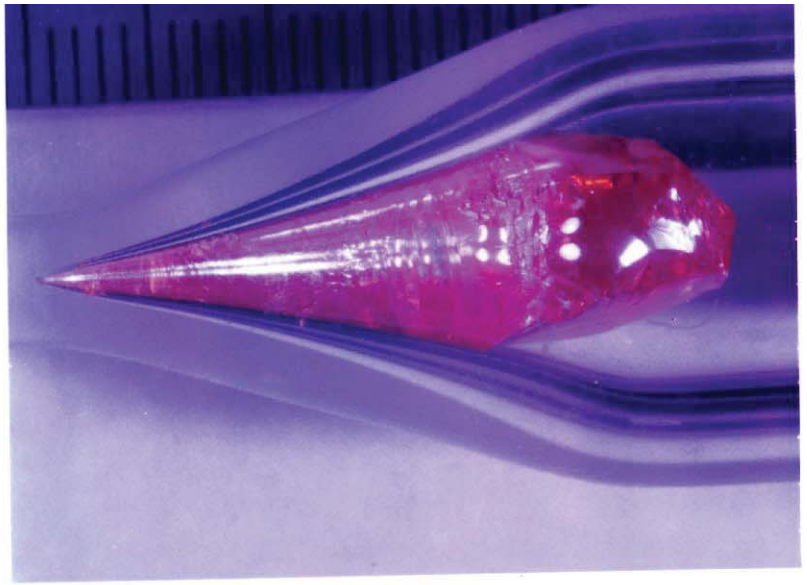

Gravity Effects on As-grown crystal morphology

- For furnace translation rates higher than the mass flux:
  - In the horizontal configuration the crystal maintained the growth surface morphological stability by (1) self-adjusting the degree of supersaturation to increase the mass flux or/and (2) by reducing the cross section area of the grown crystal.
  - In the vertical configuration the crystal growth surface became morphologically unstable with voids and pipes embedded.

ZnSe-47H 7.5 mm/day

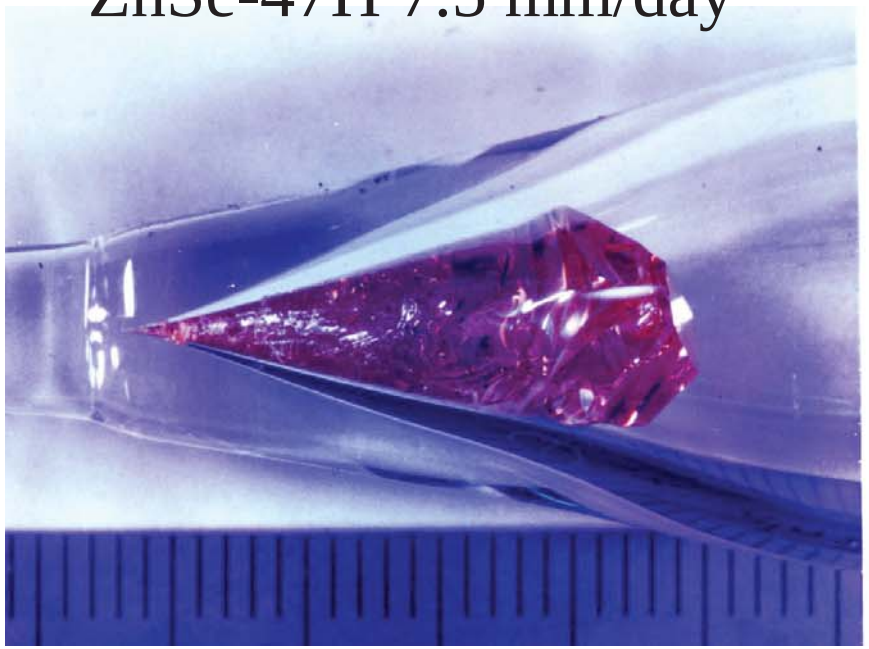

ZnSe-35V 11.4 mm/day

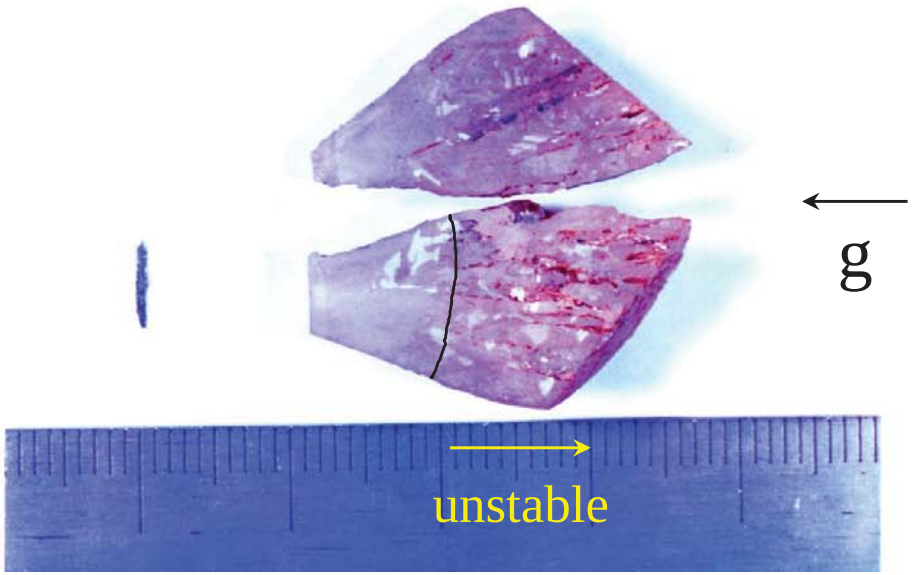

Morphologies of Seeded Vertically Grown ZnSe Crystals

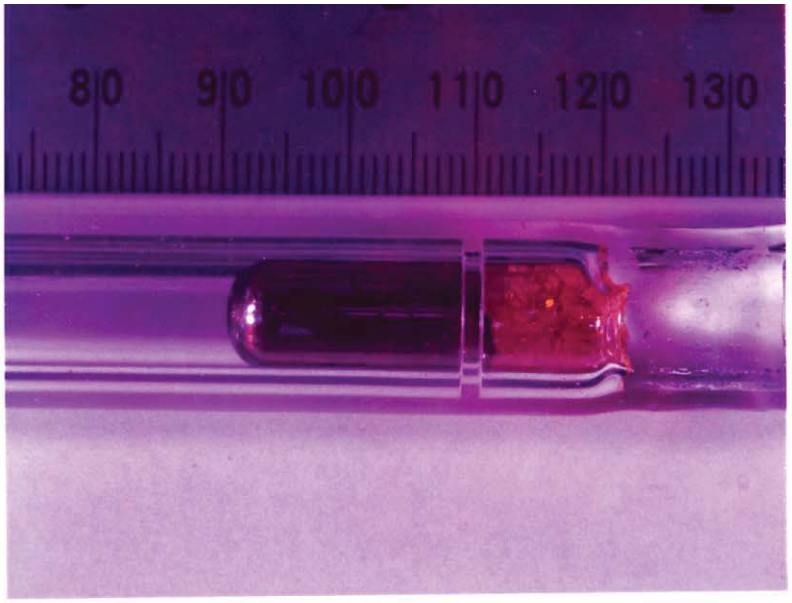

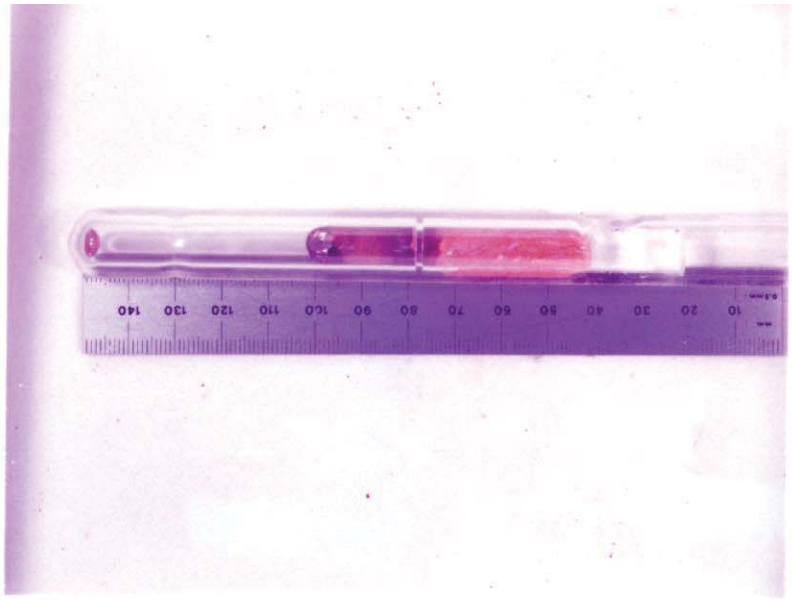

ZnSe(S)-9V

g

ZnSe(S)-12V

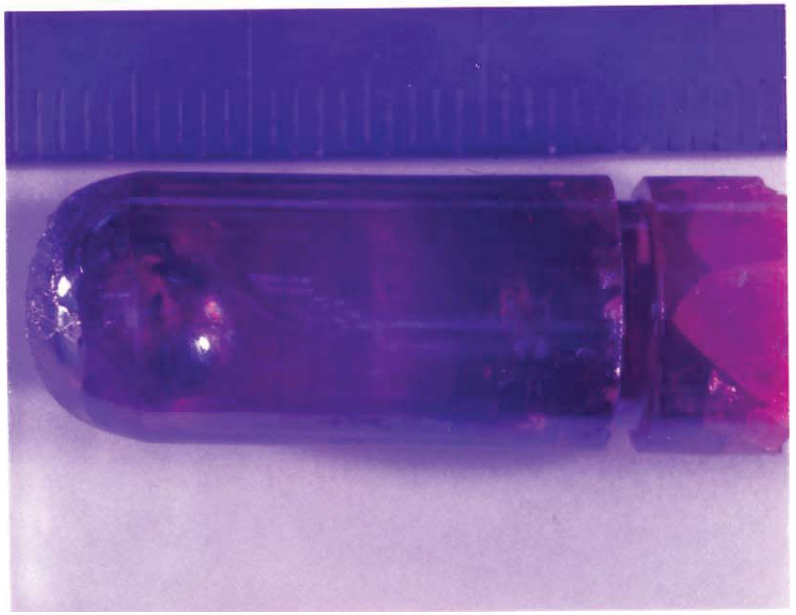

Morphologies of the Seeded Horizontally Grown ZnSe crystals

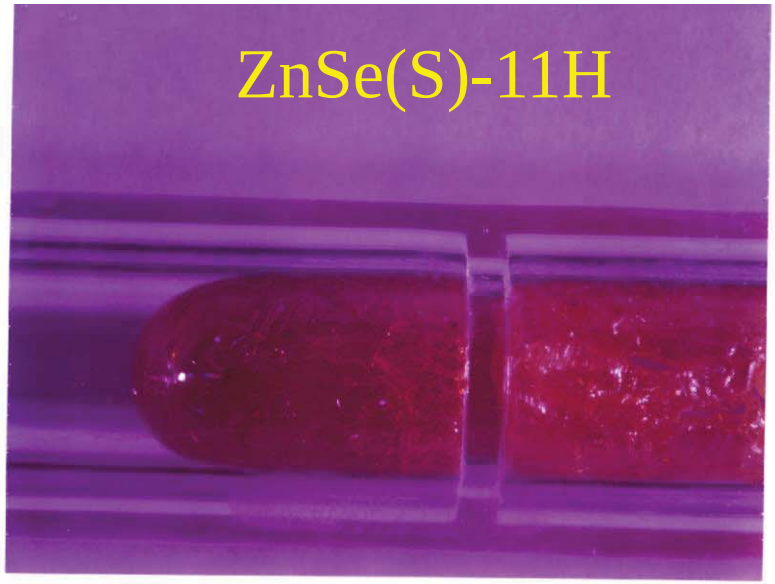

g x

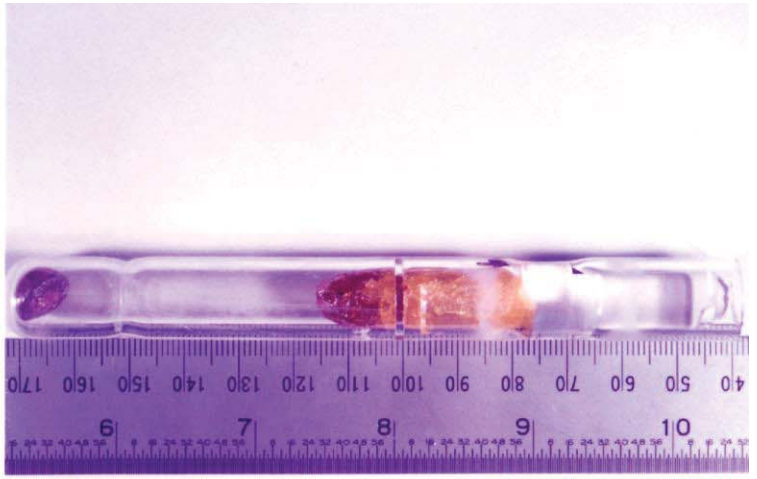

ZnSe(S)-8H

g

ZnSe(S)-13H

g

Gravity Effects on Impurities and Defects Distribution

I. Results from SIMS mappings :

For the horizontally grown self-seeded ZnSe crystal [Si] and [Fe] showed clear segregation toward the bottom on the wafer cut axially along the growth axis.

For the vertically grown seeded ZnSe crystal [Si] and [Cu] showed segregation toward the edge of the wafer cut perpendicular to the growth axis .

II. Mappings of PL near band edge intensity ratios indicated:

(1) All the horizontally-grown crystals showed the following trends in the radial and axial segregation of [Al] and [V_{Zn}]:
[Al] segregates radially toward the top and axially toward the first grown region and [V_{Zn}] segregates radially toward the bottom and axially toward the last grown region.

(2) The as-grown surface of the seeded vertically stabilized grown crystal showed [Al], [Li or/and Na] and [V_{Zn}] segregate radially toward the center.

(3) The as-grown surface of the self-seeded vertically destabilized grown crystal showed [Al] and [V_{Zn}] segregate radially without an apparent pattern.

Su et al (1999)

Impurities Distribution by SIMS (horizontally grown)

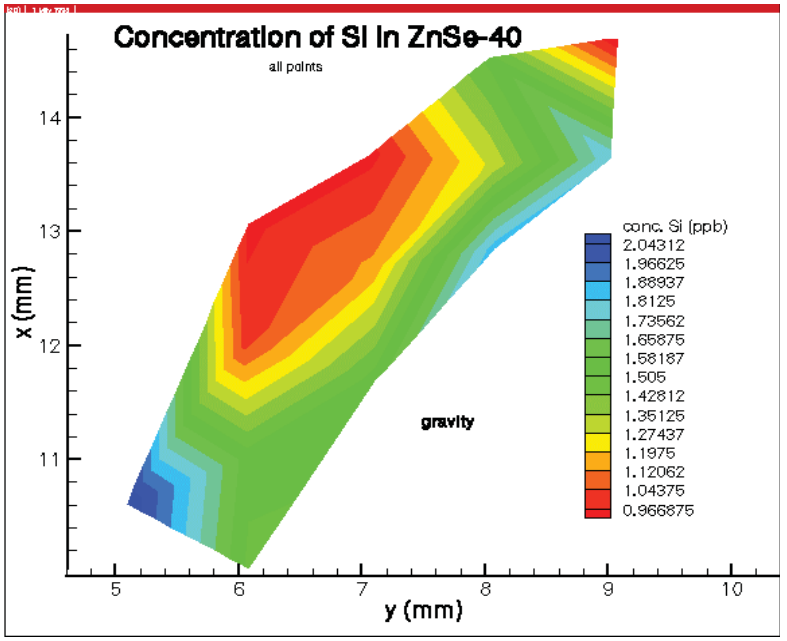

growth direction

gravity

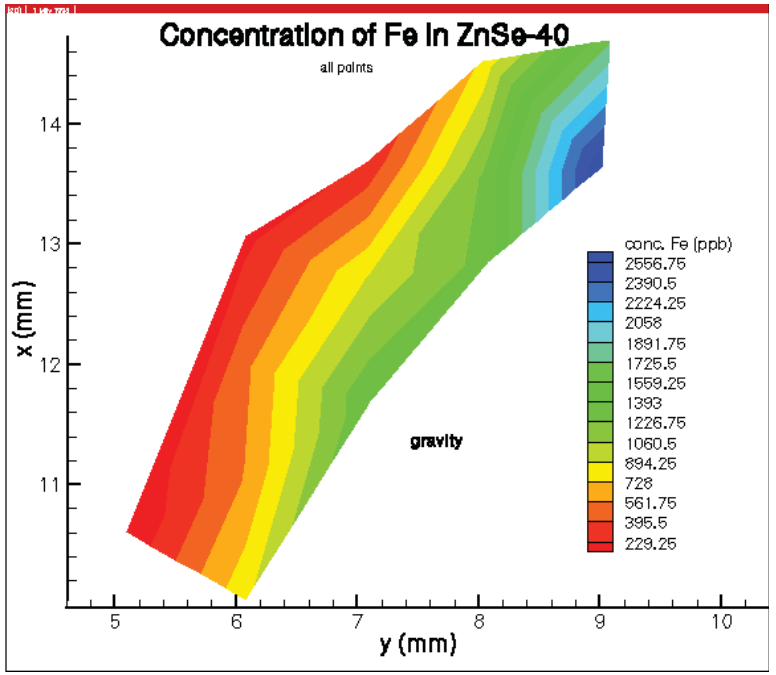

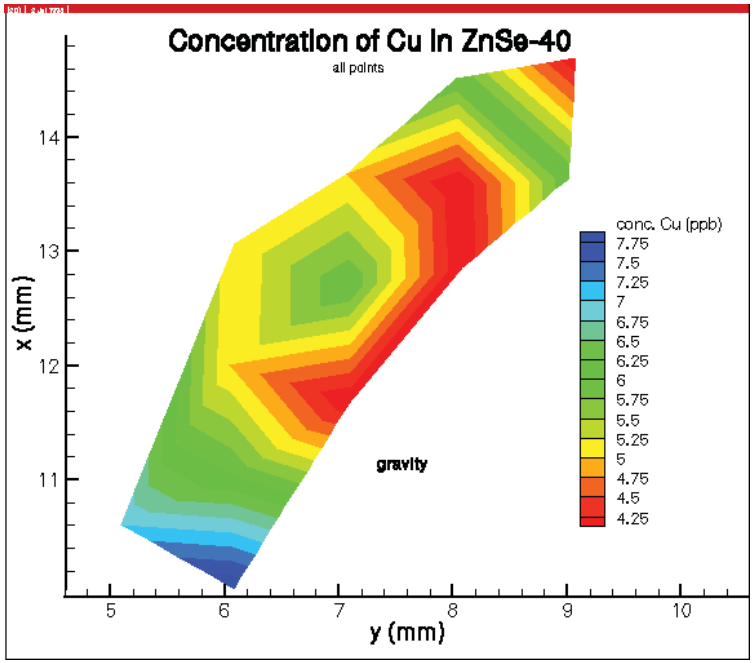

Impurities Distribution by SIMS (vertically grown)

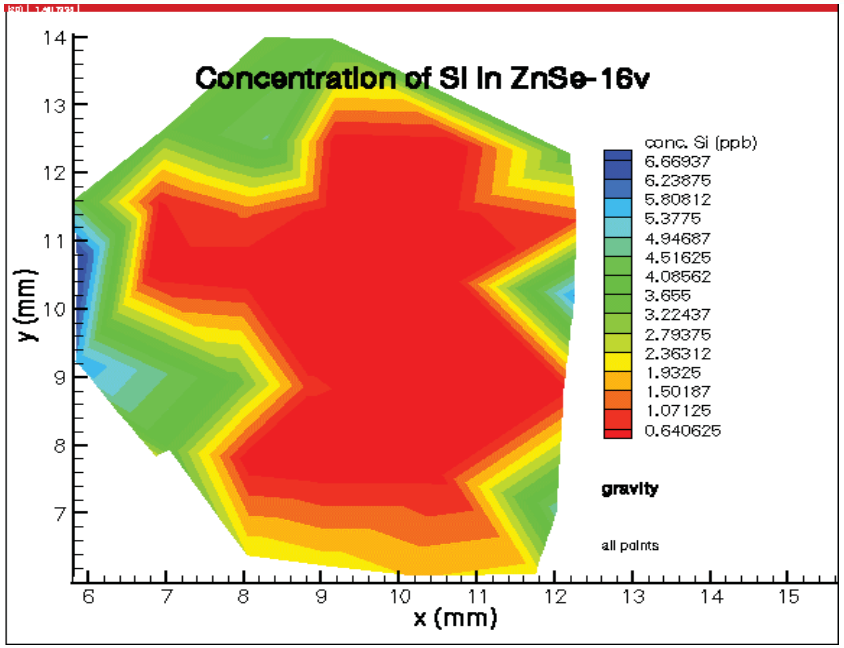

x

gravity and

growth direction

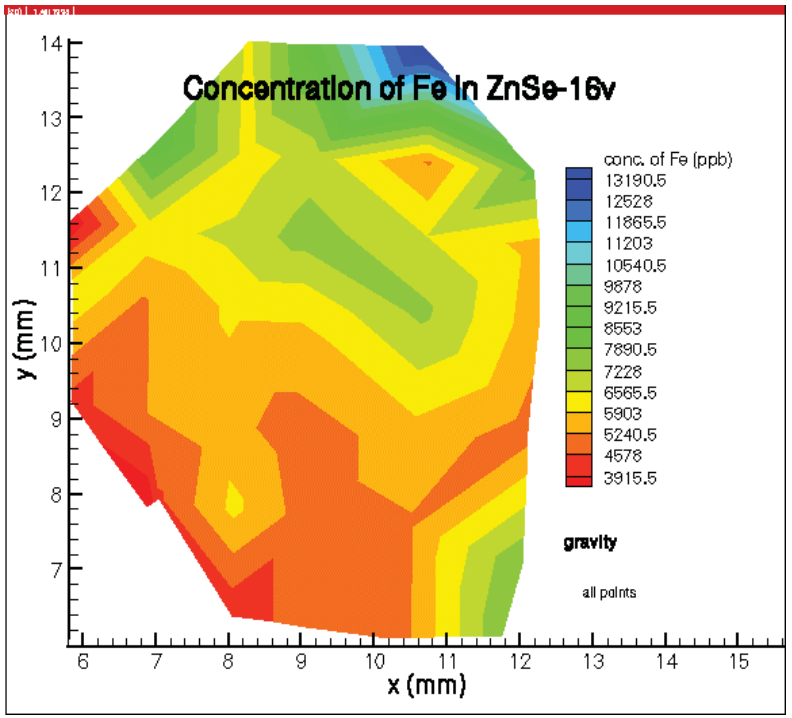

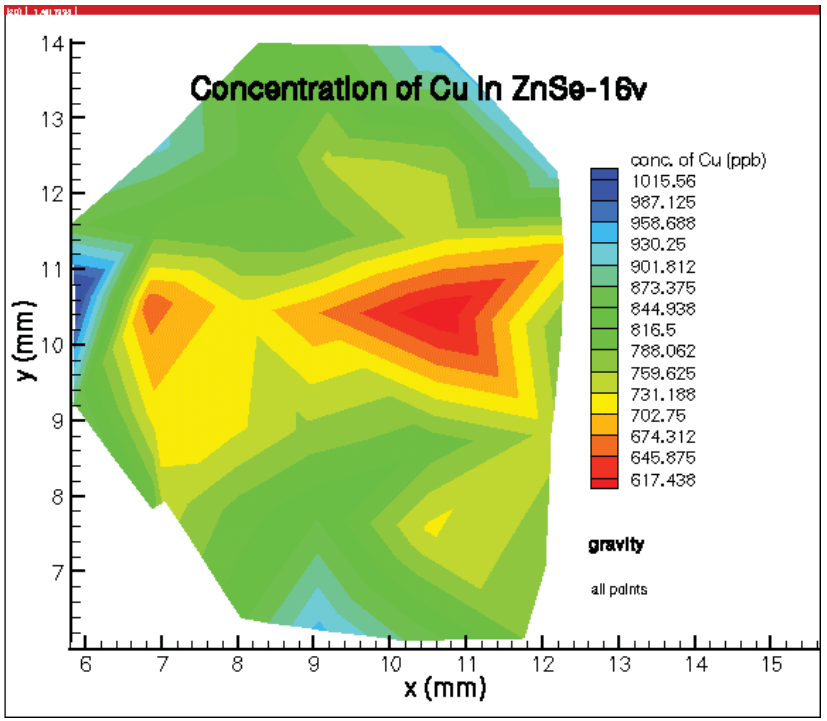

Summary on the Photoluminescence I_2 and I_1^{deep} emissions

I_2 emission:

- I_2, the exciton bound to substitutional donor, emission in our ZnSe samples can be attributed mainly to Al impurity, with $A(I_2)/A(F_x) = 4.88$ corresponding to 1700 ppb, atomic, or 7.46×10^{16} cm^{-3}.
- Isshiki et al. (1991) gave the expression between intensity ratio $(I_2)/(I_{Fx})$ and N_D:

  $$\log_{10}(I_2/I_{Fx}) = -22.0775 + 1.46268 \log_{10}N_D(cm^{-3})$$
- Therefore, $(I_2/I_{Fx}) = 82\,[A(I_2)/A(F_x)]$

I_1^{deep} emission:

- I_1^{deep} is related to exciton bound to V_{Zn} deep acceptor and $[V_{Zn}]$ is proportional to $A(I_1^{deep})/A(F_x)$.
- The reaction during Zn vapor annealing:

  $$Zn_{Zn} \quad V_{Zn} + Zn(g)$$

  $$K = [V_{Zn}] \times P_{Zn} = K_1 A(I_1^{deep})/A(F_x) \times P_{Zn}$$
- The ZnSe samples were annealed at 1104 ^oC:

1. $A(I_1^{deep})/A(F_x) = 7.52$ when sample is in equilibrium with $P_{Zn} = 6.1 \times 10^{-3}$ atm ($\alpha = 6.05$) $A(I_1^{deep})/A(F_x) \times P_{Zn} = 0.0459$ atm.
2. $A(I_1^{deep})/A(F_x) = 5.18$ when sample is in equilibrium with $P_{Zn} = 9.0 \times 10^{-3}$ atm ($\alpha = 19.43$) $A(I_1^{deep})/A(F_x) \times P_{Zn} = 0.0466$ atm

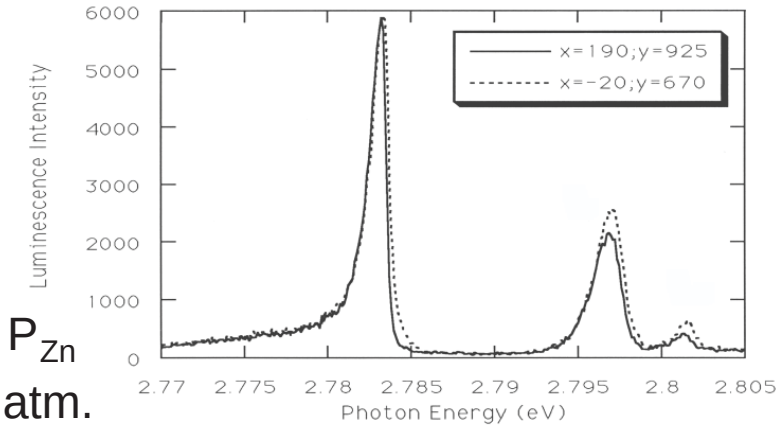

Distribution of $[V_{Zn}]$ and [Al] in ZnSe (horizontally grown)

$[V_{Zn}]$

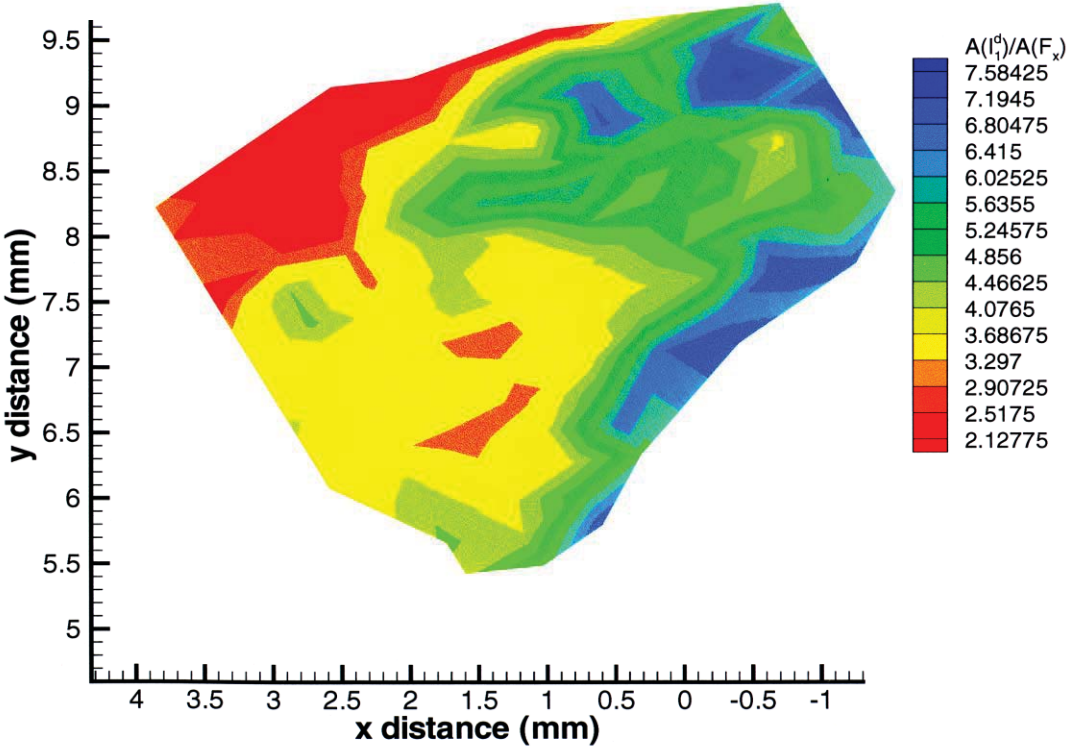

[Al]

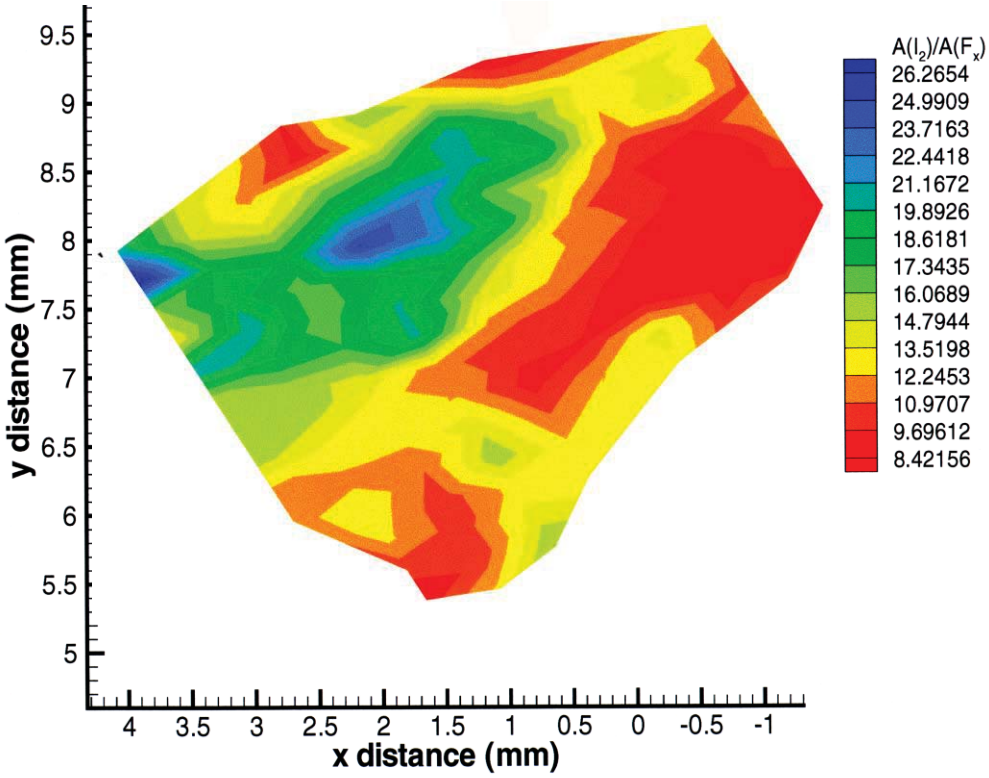

gravity

growth direction

Distribution of $[V_{Zn}]$ and [Al] in ZnSe (horizontally grown)

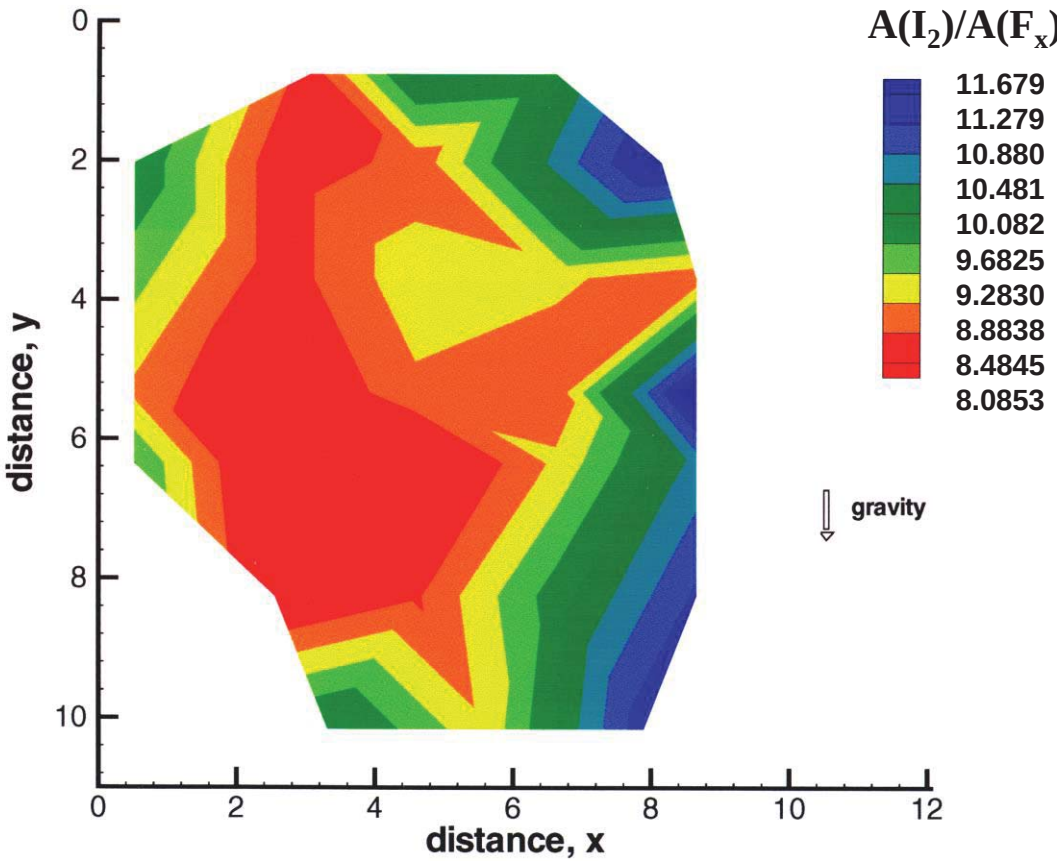

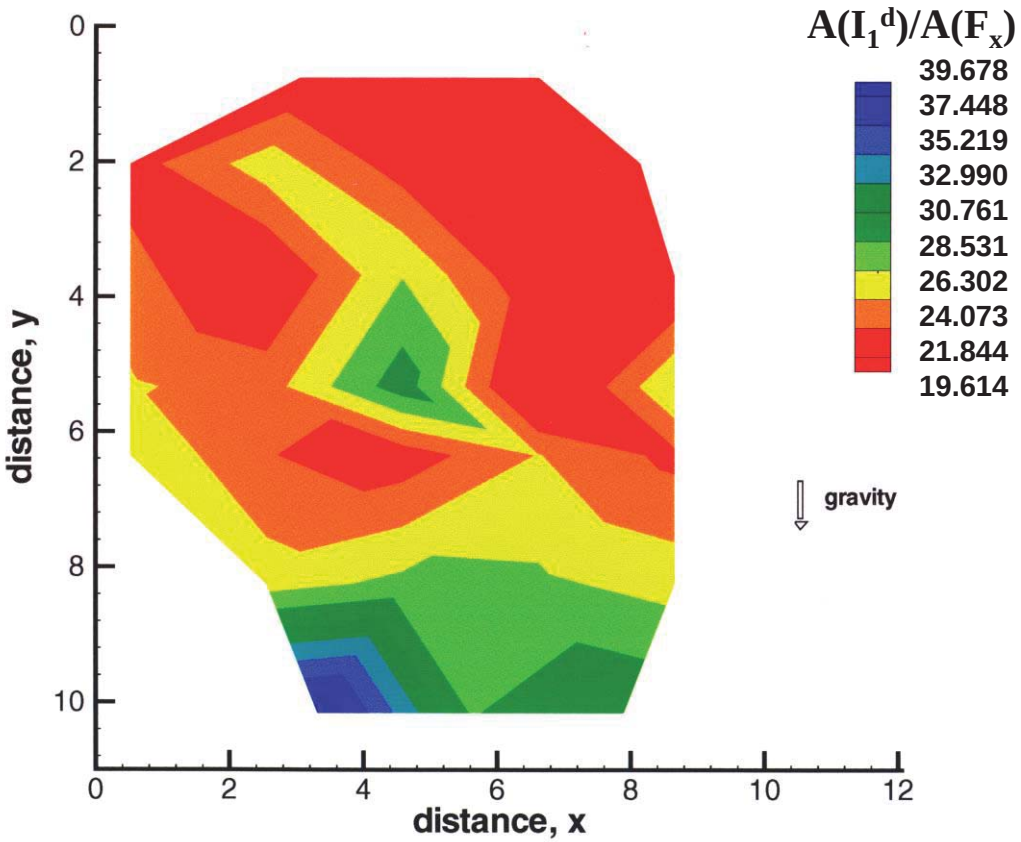

gravity

x

growth direction

Distribution of [V_{Zn}] and [Al] in ZnSe (vertically grown)

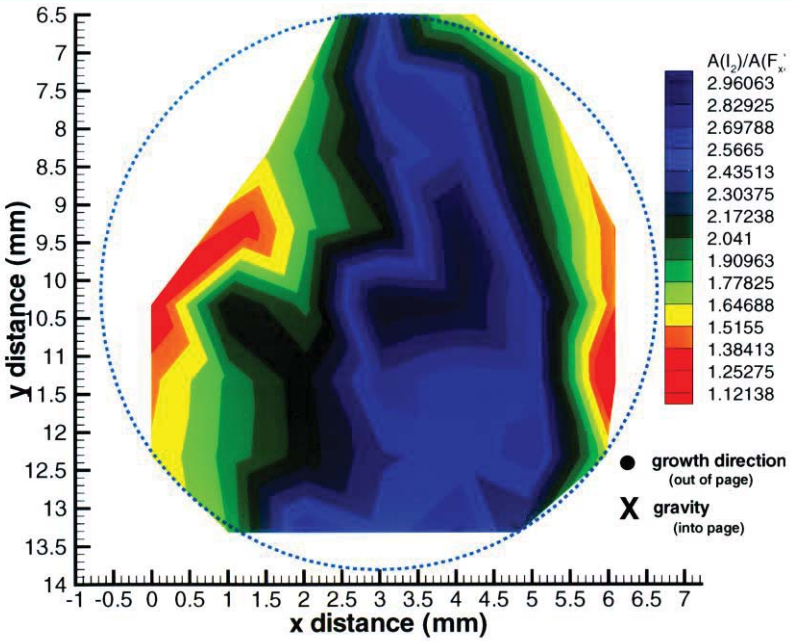

Vertical stabilized configuration

$A(I_1^d)/A(F_x)$

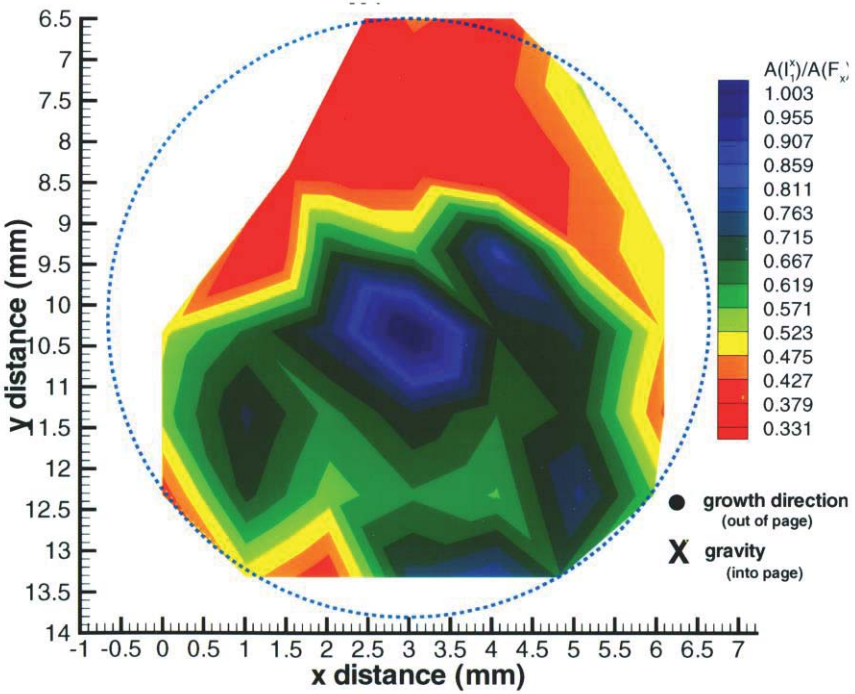

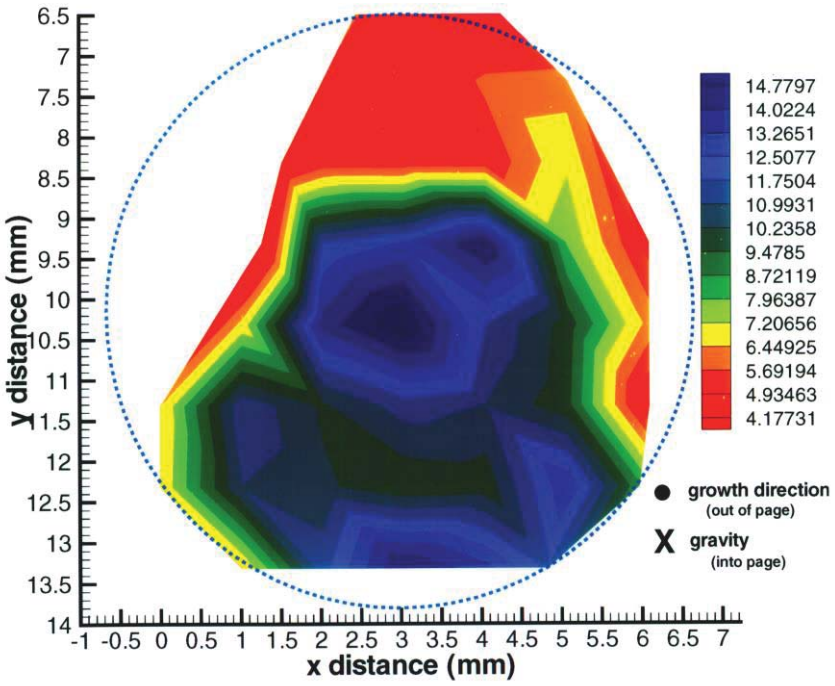

Distribution of $[V_{Zn}]$ and [Al] in ZnSe (vertically grown)

Vertical destabilized configuration

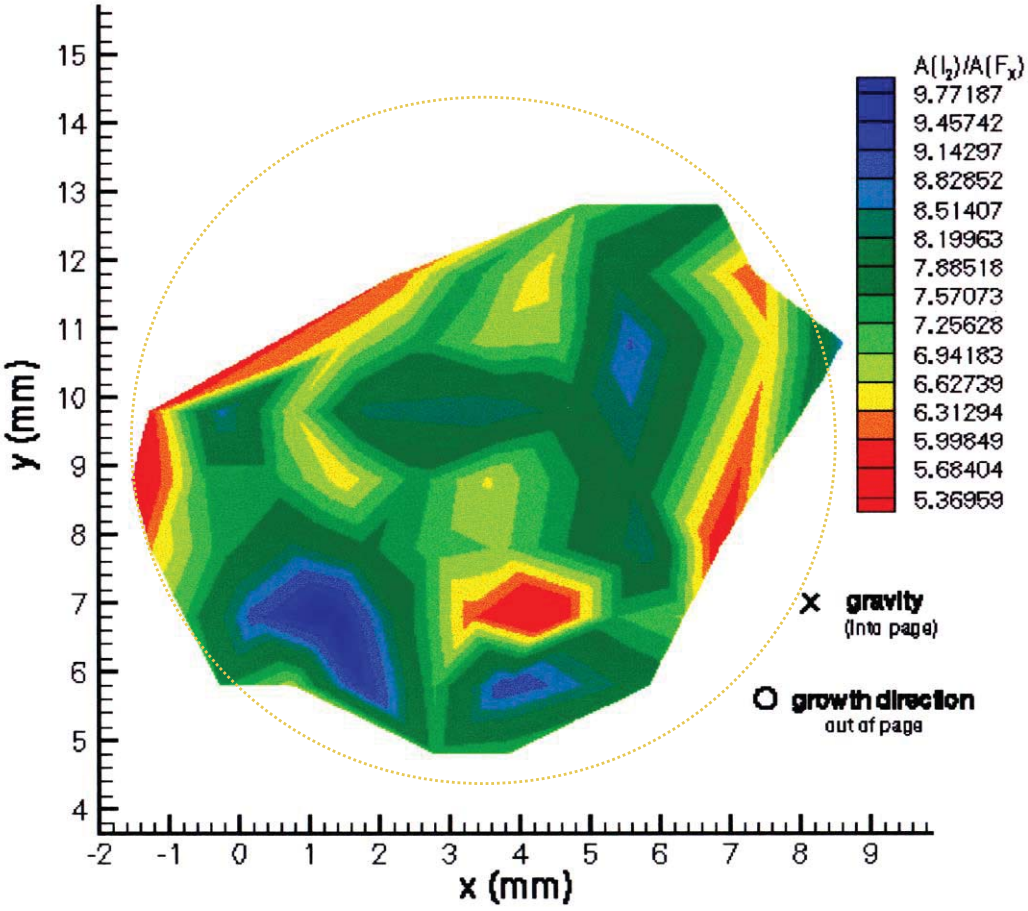

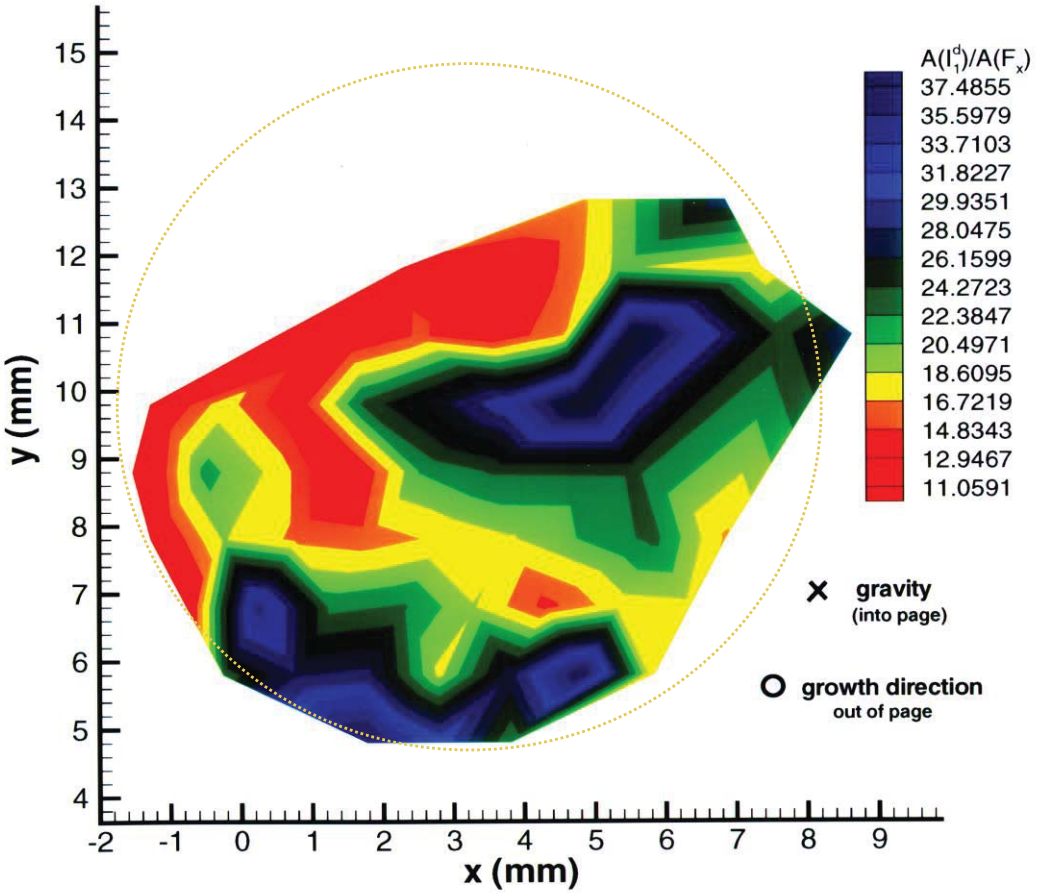

Synchrotron X-ray Transmission Topography of ZnSe wafer

Thin twin lamellae (TL) and three sets of (111) slip bands (S) originating from the lateral twin boundaries.

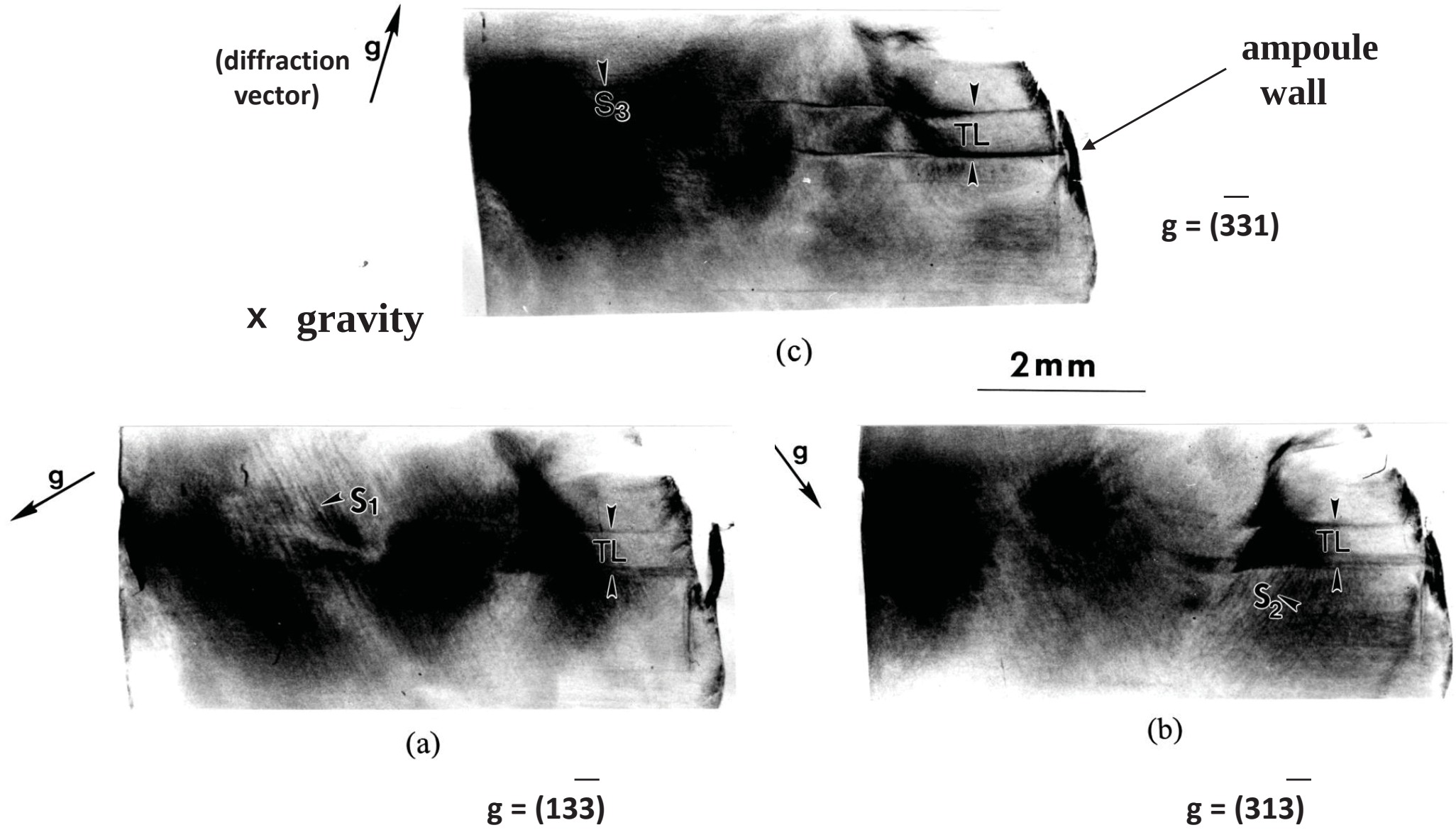

Reflection Topograph of ZnSe-43H as-grown Facet

Reflection SWBXT image on the as-grown facet of ZnSe-43H showed areas of twins. The crystalline quality is generally good except that the upper region, where the crystal started to grow into full diameter and away from the ampoule wall, showed lattice strain.

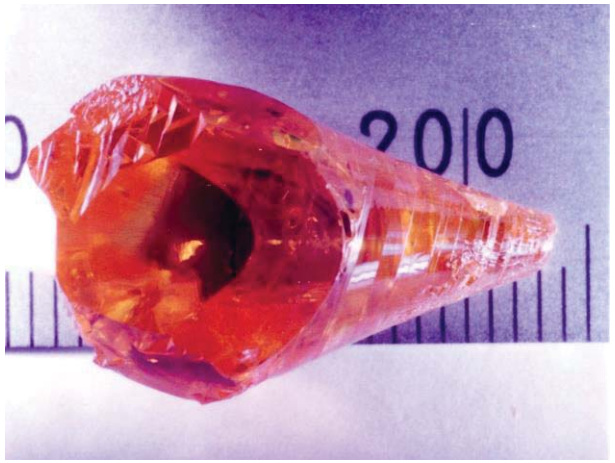

gravity ↓

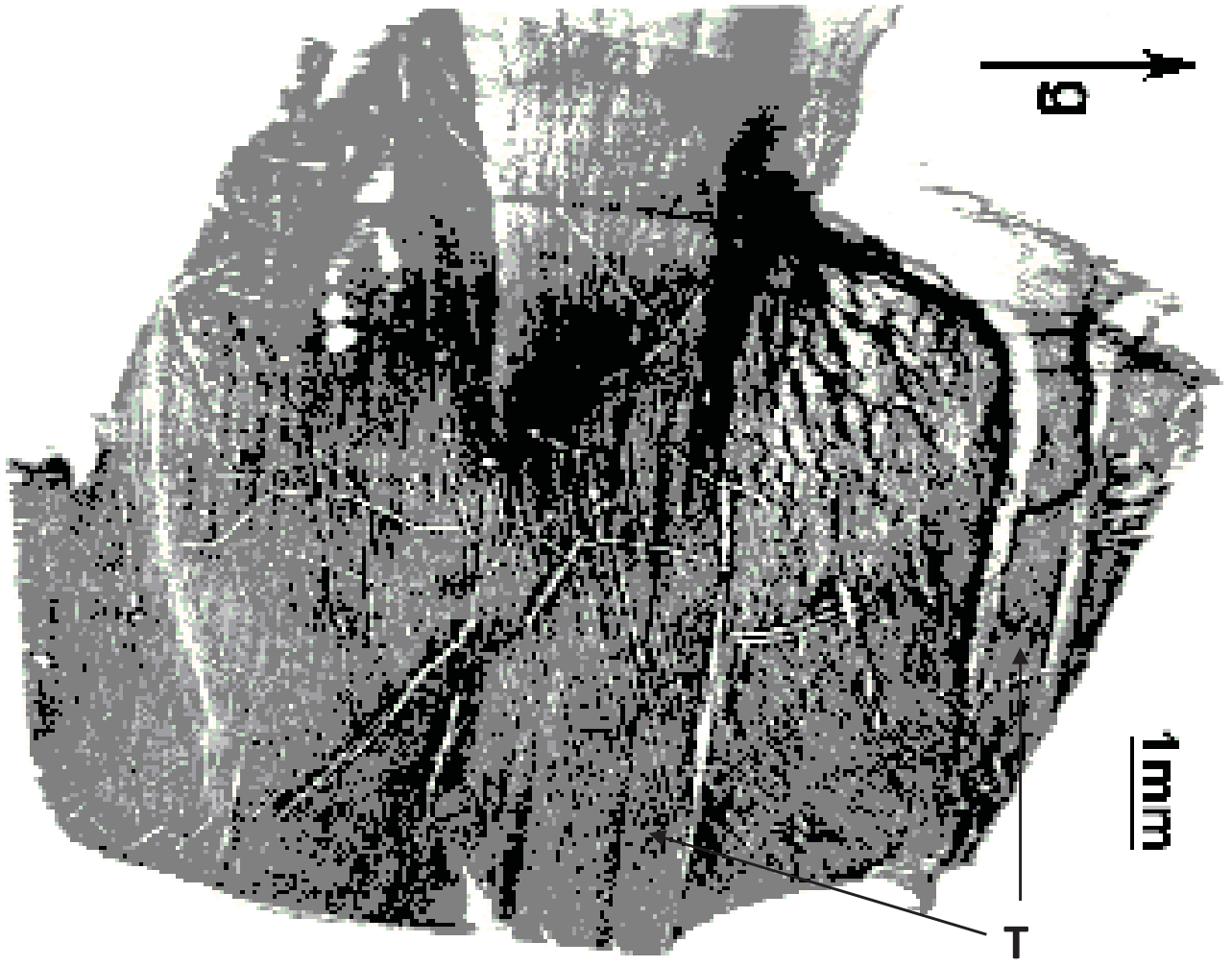

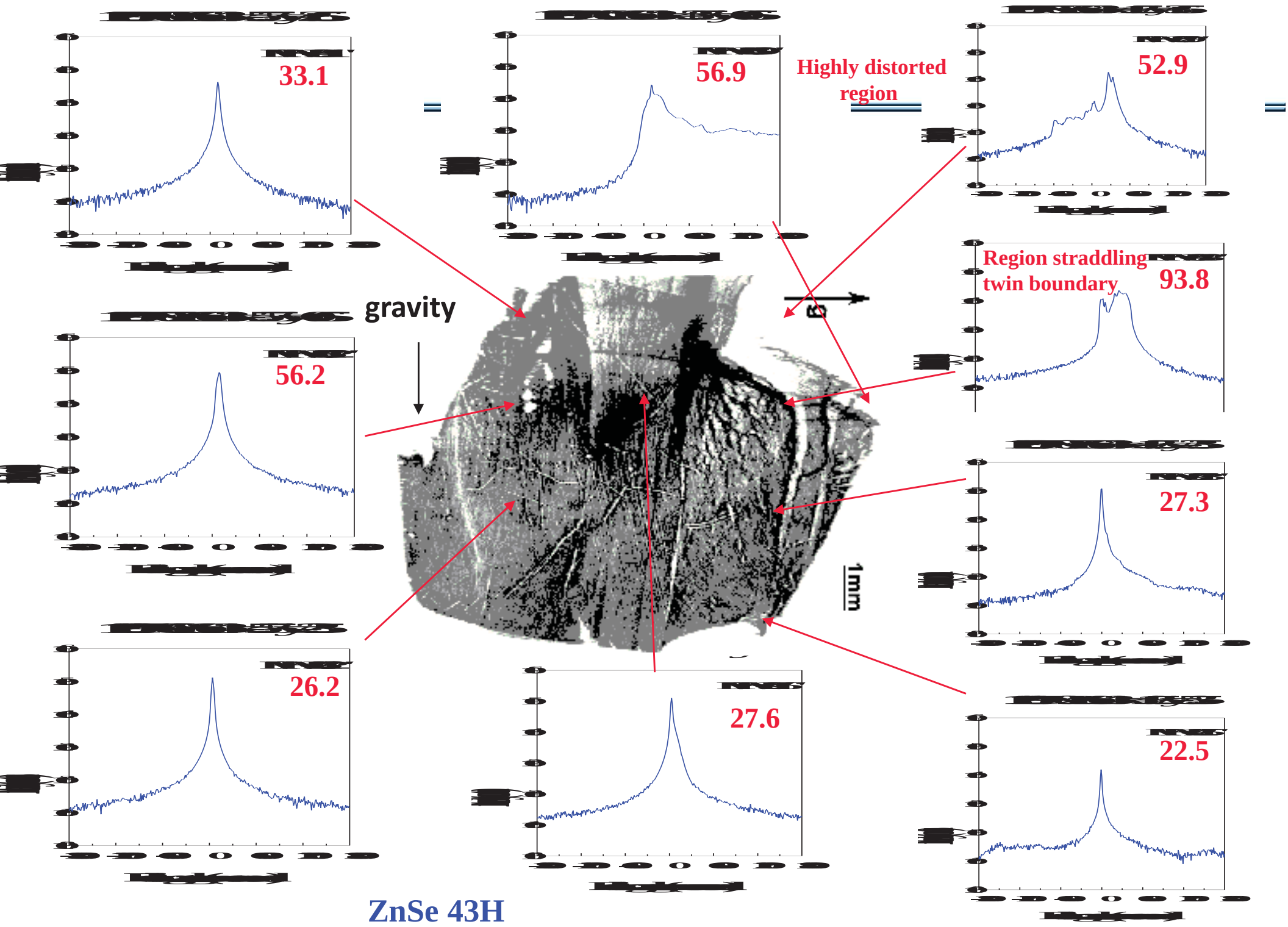
33.1
56.9
52.9
56.2
93.8
27.3
26.2
27.6
22.5
Highly distorted region
Region straddling twin boundary
gravity
1mm
ZnSe 43H

In-situ optical monitoring during crystal growth

- Optical absorption for partial pressure measurements along the length of the growth ampoule to measure vapor phase transport species distribution
- Optical interferometry to measure seed thermal etching, instantaneous growth rate and the evolution of surface topography
- Visual observation of the growth evolution

Ampoule Design for in-situ Optical Monitoring

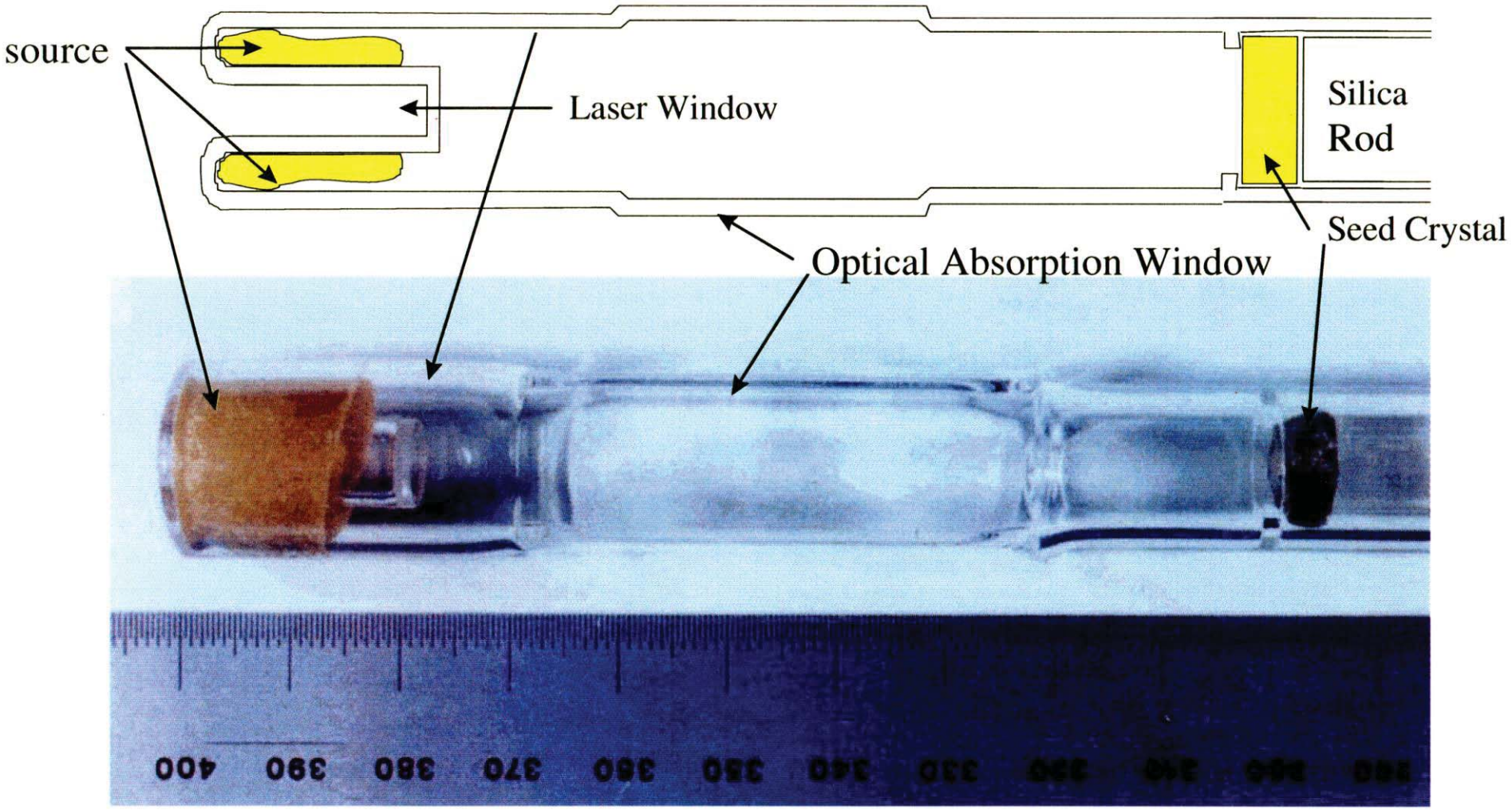

Measured Partial Pressure as a Function of Time

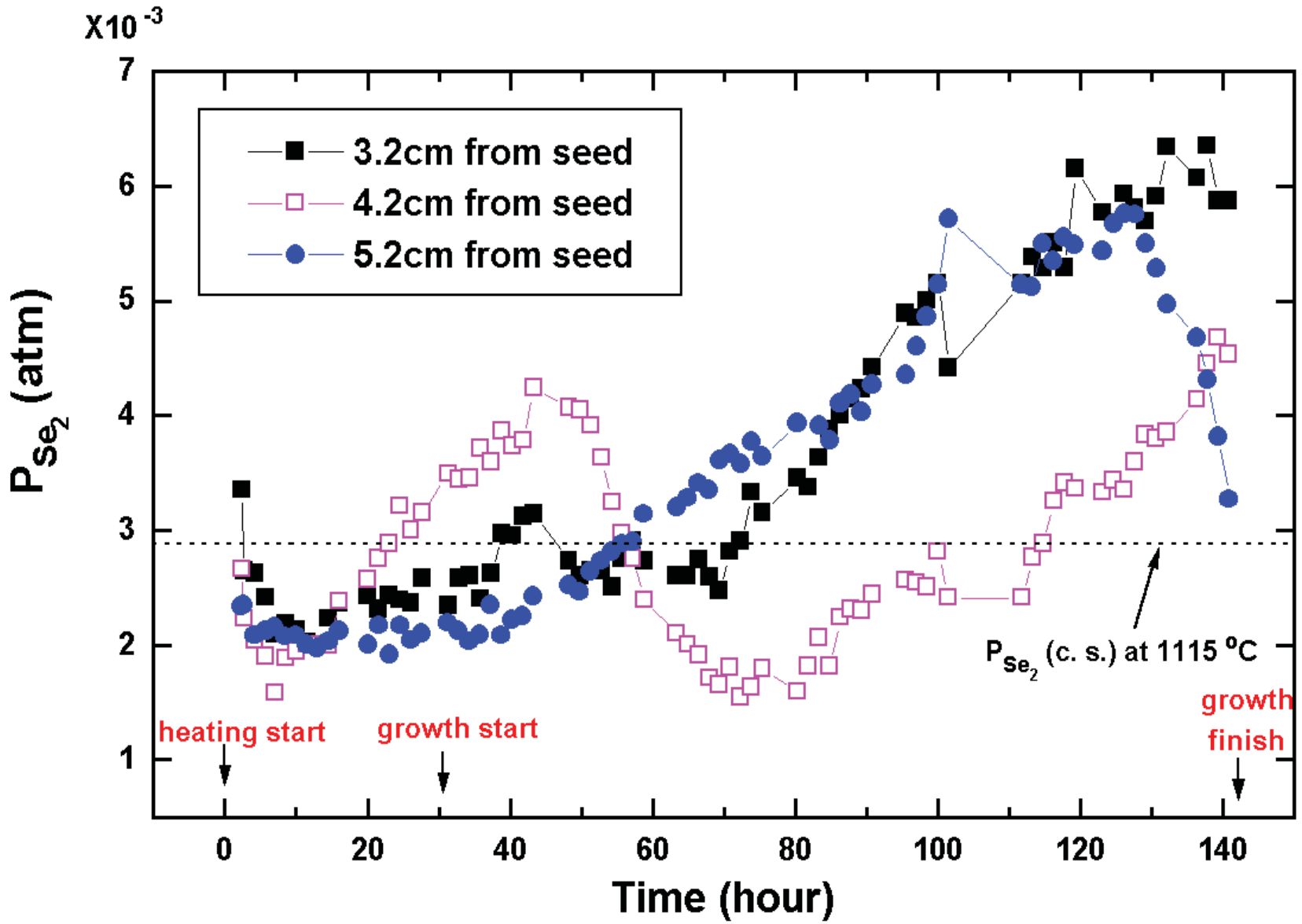

Interferometry Results from Seed Crystal Surface

(Room Temperature)

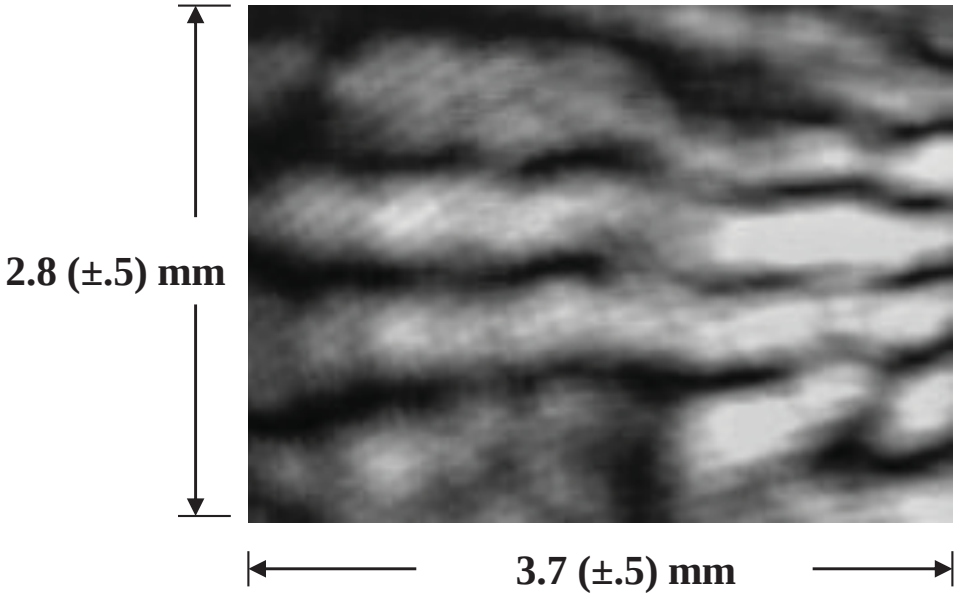

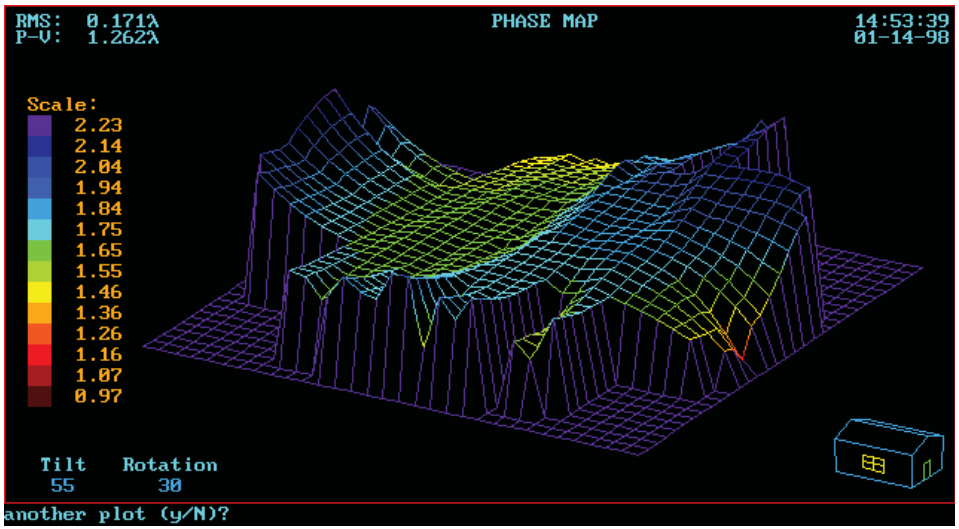

Fringes from Fabry-Perot Interferometer

Fast/Vai Phase Map of Crystal Surface, (from Fringes)

Interferometry Results from Seed Crystal Surface

(at 1120°C)

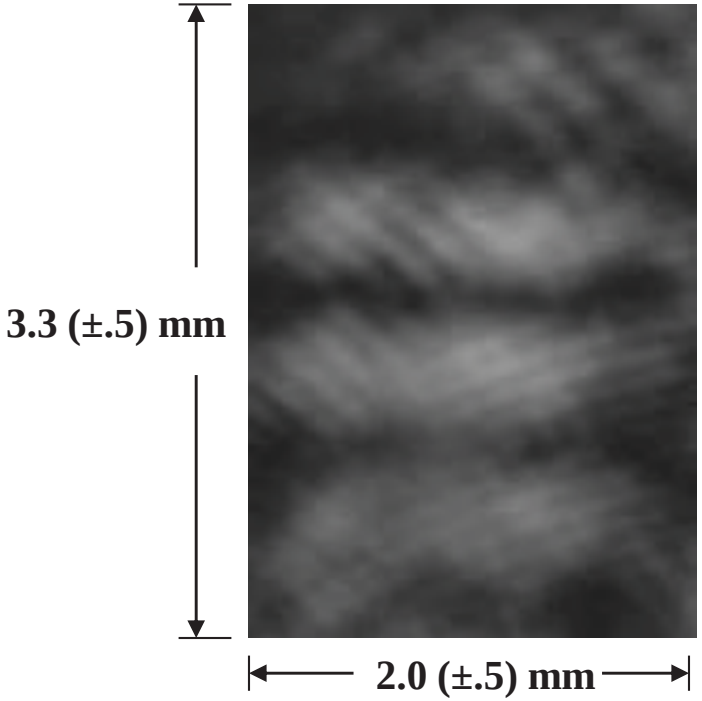

Fringes from Fabry-Perot Interferometer

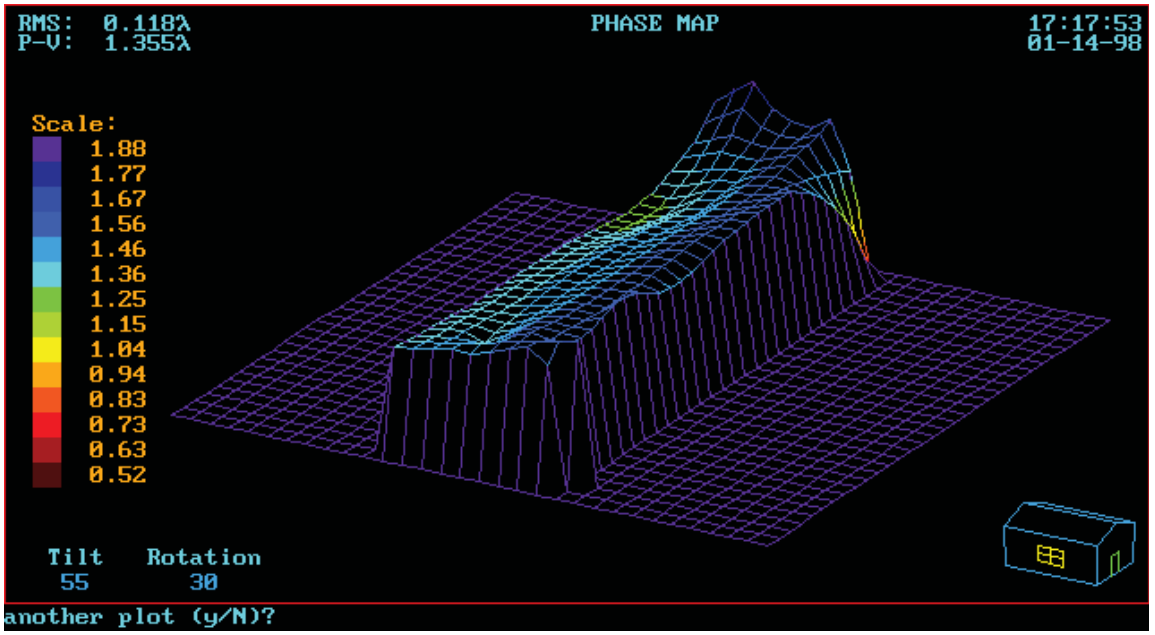

Fast/Vai Phase Map of Crystal Surface, (from Fringes)

Synchronized plots of sample temperature and the measured thermal expansion

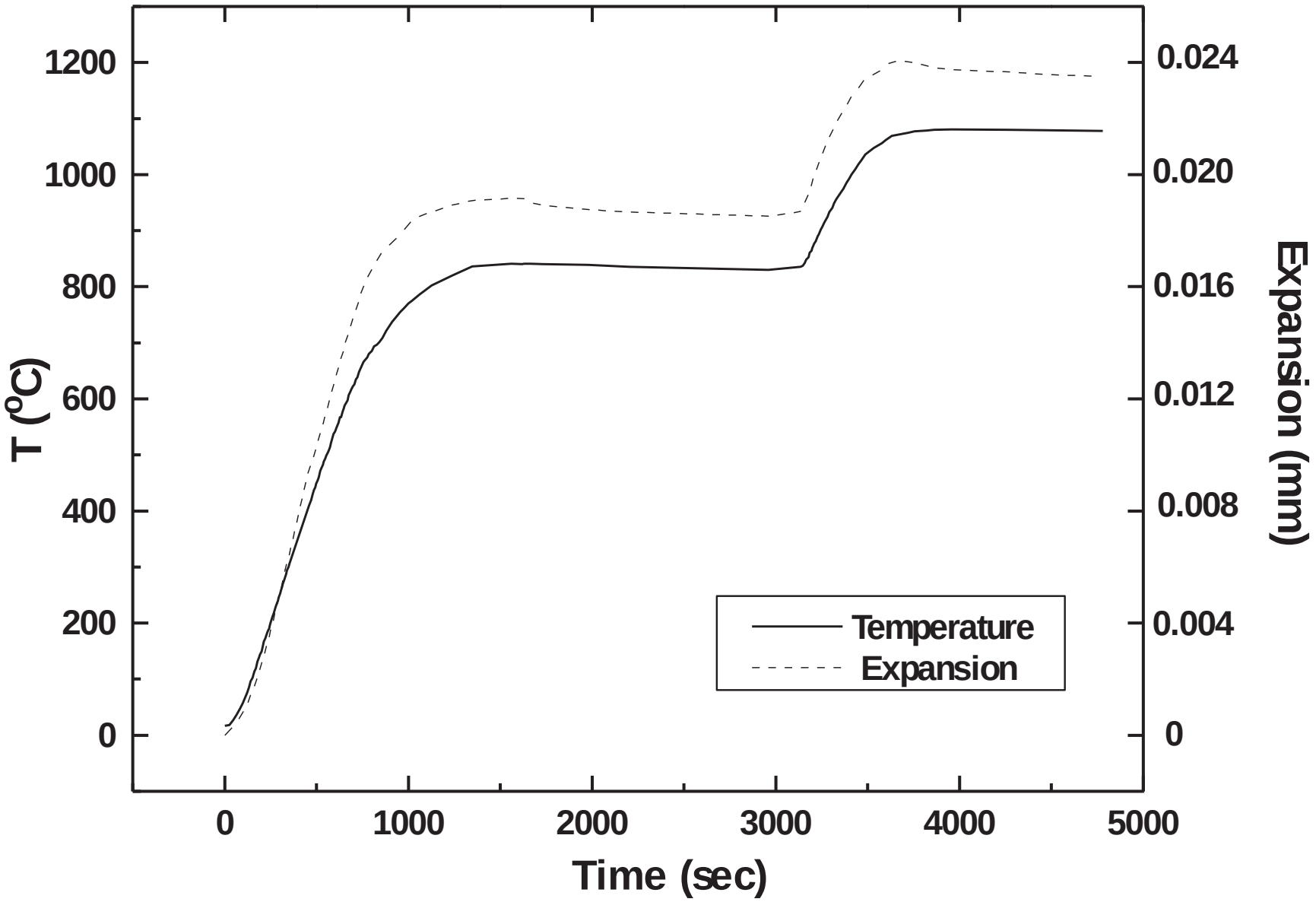

Thermal Expansion Coefficient of ZnSe from Interferometry

Expansion $\Delta L = n(\lambda/2)$ $\lambda = 632.8nm$ $L_0 = 4.5mm$

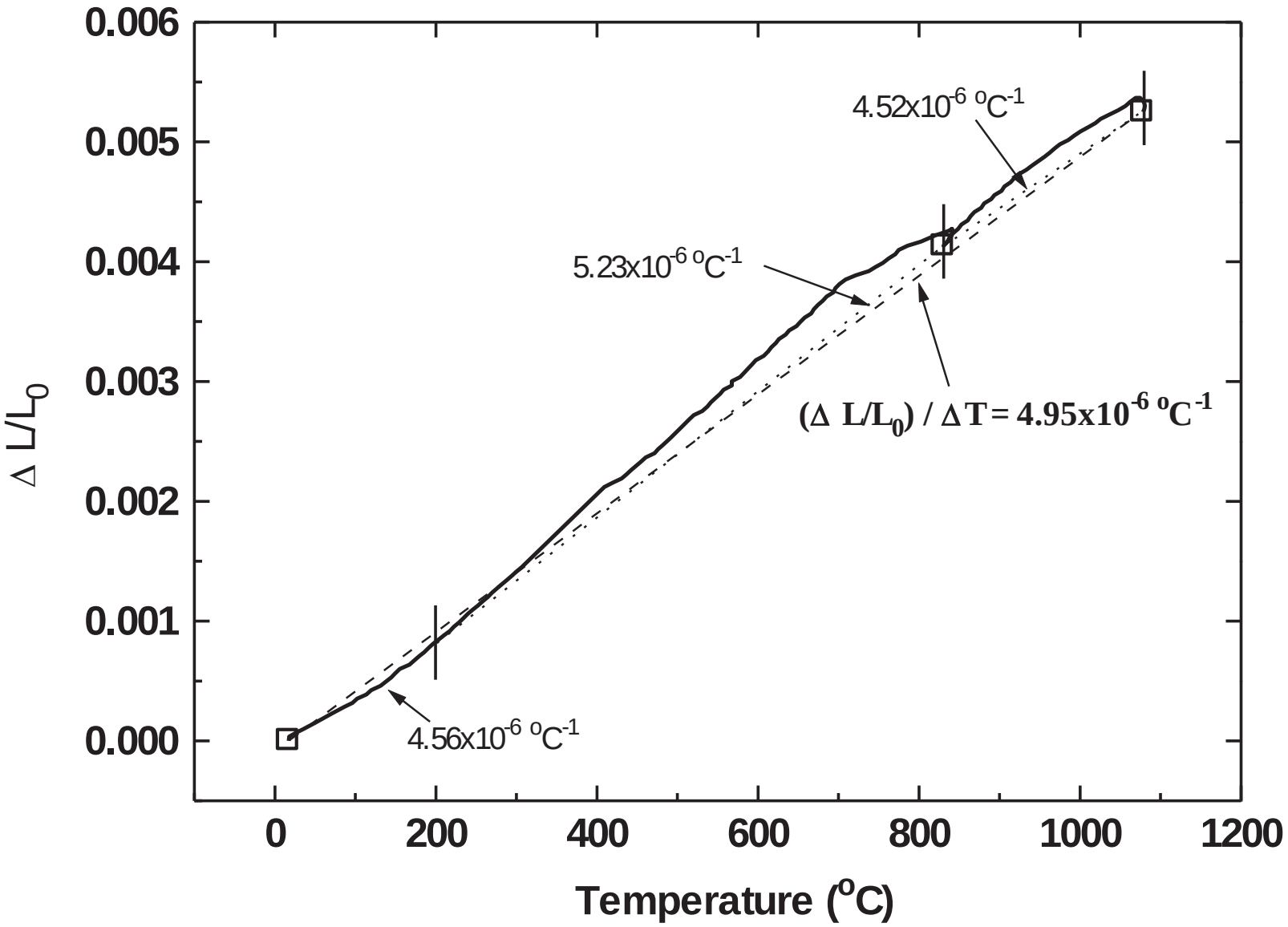

Numerical Modeling of Physical Vapor Transport

- Two dimensional and three dimensional calculations
- Finite element technique - Fidap code
- Thermal and Species induced buoyancy forces
- Compressible or Boussinesq model
- Benchmark -2D (H_2-I_2 system - PVT growth)
- ZnSe calculations with residual gas
- Benchmark -3D (Natural convection in a cylinder)
- 3-D ZnSe calculations with residual gas
- Ongoing and future work

Ramachandran et al. (2000)

The Physical Model

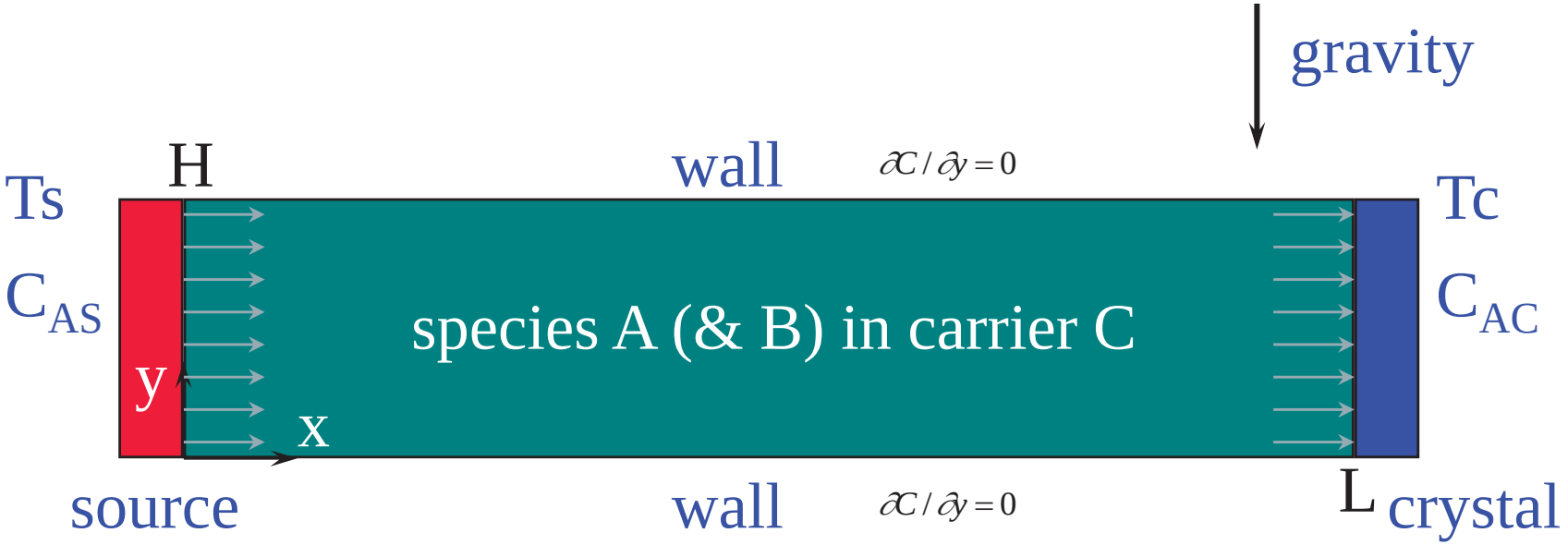

wall temperature

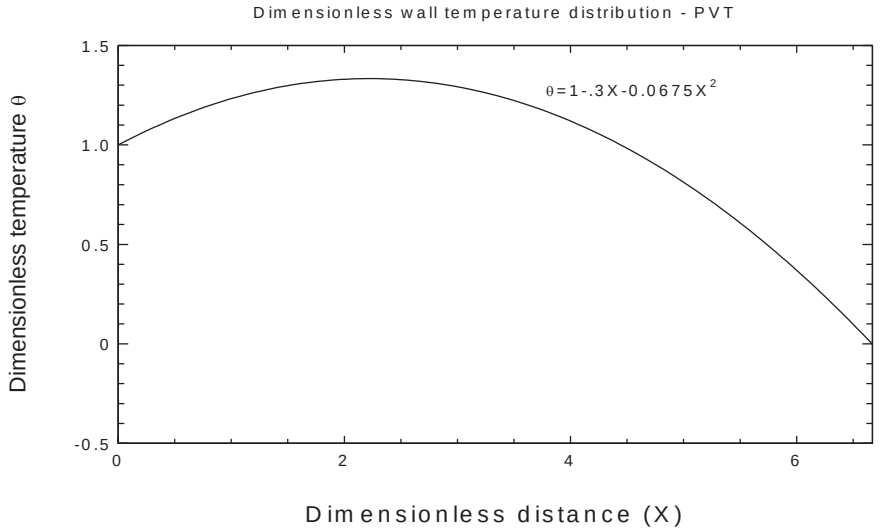

Benchmark → the H_2-I_2 System

- benchmark calculations by Rosenberger et al. (J. Crystal Growth 51 426 1981; 67 241 1984; 118 49 1992)
- source temperature Ts=370.5 K
- crystal temperature Tc=358.1 K
- ampoule pressure : 100 torr
- I_2 (M=254) is the deposited species and H_2 (M=2.016) is inert
- 2-d Cartesian system
- linear wall temperature
- quasi-compressible and Boussinesq calculations
- Peclet number analysis, Pe ~ 1 for diffusive flow
- growth rate results

3-D Computational Grid and Code Validation Results

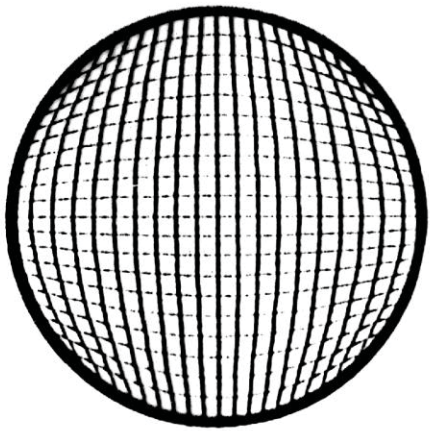

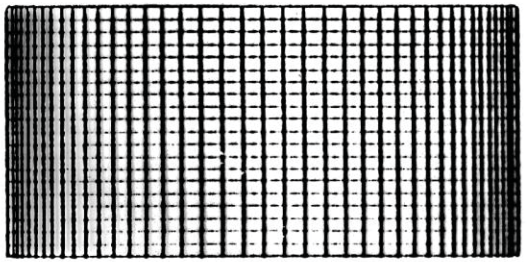

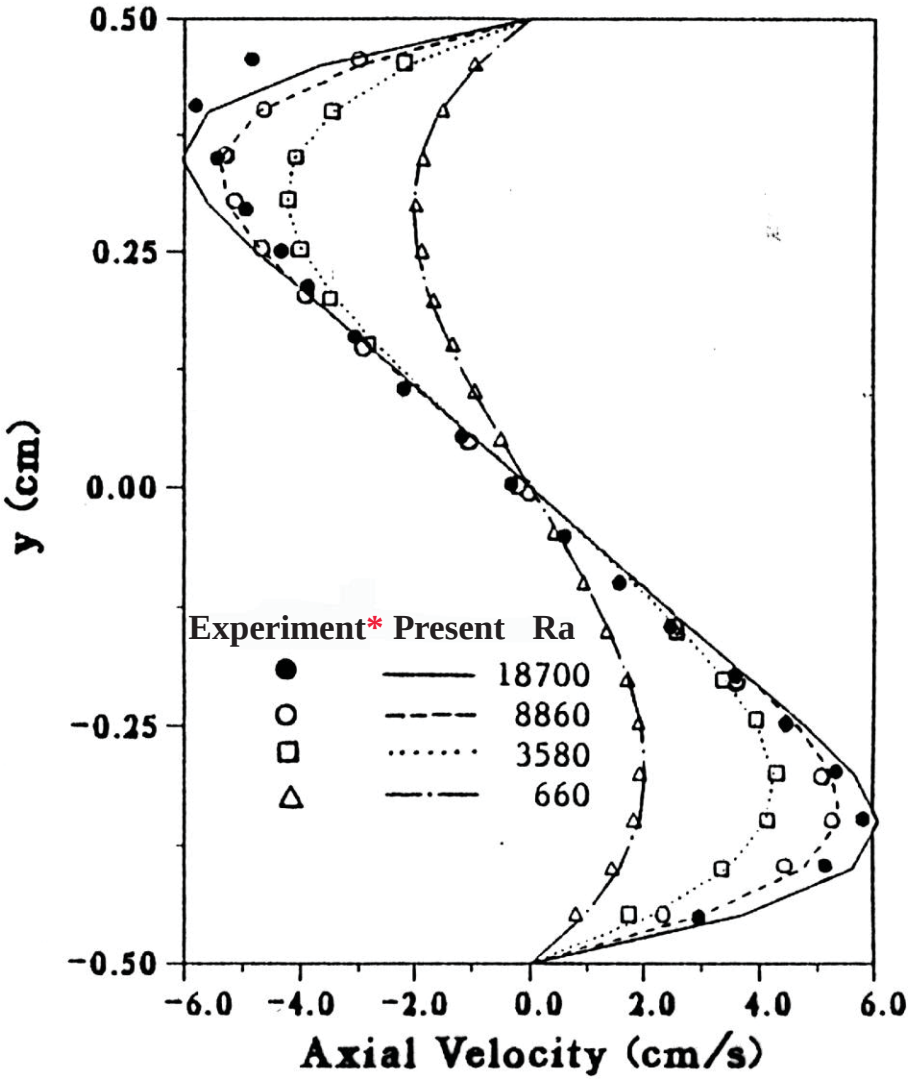

* Schiroky and Rosenberger (1984)

Parameters of ZnSe System with Residual Gas

$\alpha = 2.9$

- density, 1.2×10^{-5} g/cm^3
- dynamic viscosity, 4.3×10^{-5} Pa-s
- kinematic viscosity, 36 cm^2/s
- diffusivity, Zn in N_2, 64.59 cm^2/s
- diffusivity, Se_2 in N_2, 71.46 cm^2/s
- thermal expansion coefficient, 7.1×10^{-4} K^{-1}
- Prandtl number, 0.439
- Schmidt number, $Sc_{zn} = 0.557$
- Schmidt number, $Sc_{se} = 0.503$

Velocity Difference Plots - procedure

- calculations for pure diffusion limited conditions, 0g
- calculations for other g conditions, a conditions, etc.
- calculate differences in axial (u) and transverse (v) velocities at all identical grid locations between previous steps; e.g. U(0g) - U(1g) and V(0g)-V(1g)
- contour the velocity differences and plot
- determine g-sensitivity
- Note: all calculations were using the Boussinesq approx.

conventions:

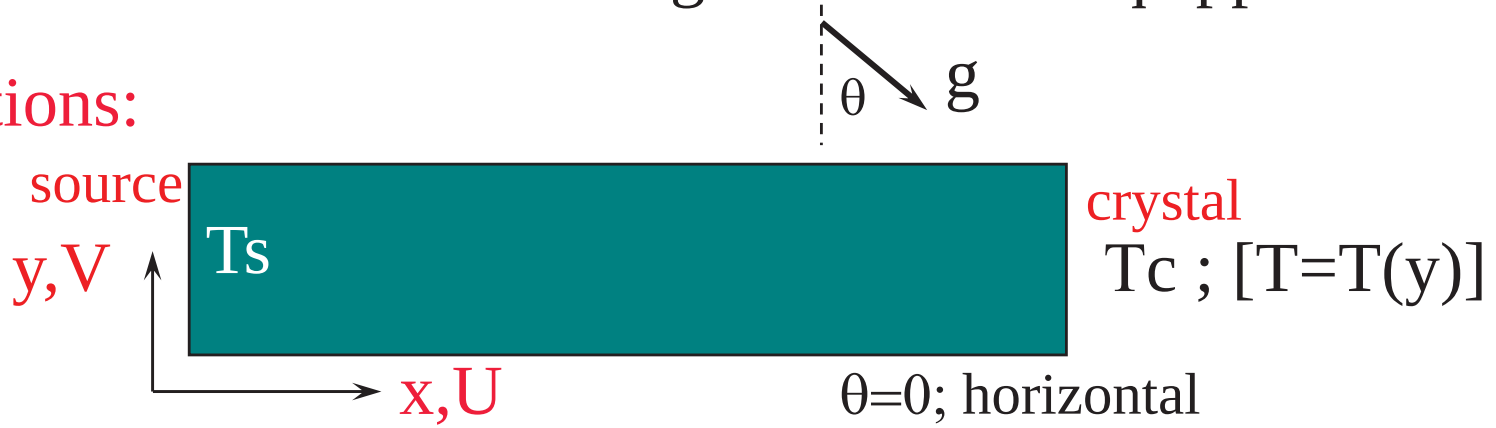

θ=0; horizontal
θ=90; vertical stabilized
θ=270; vertical destabilized

Gravity Effect on Velocity Difference (horizontal case)

- g-effects with constant crystal temperature , Tc.
  ΔU~ 0.3 mm/s; ΔV~ 50 μm/s

- g-effects with crystal temperature variation, Tc = Tc(y).
  ΔU~ 0.3 mm/s; ΔV~ 43.75 μm/s

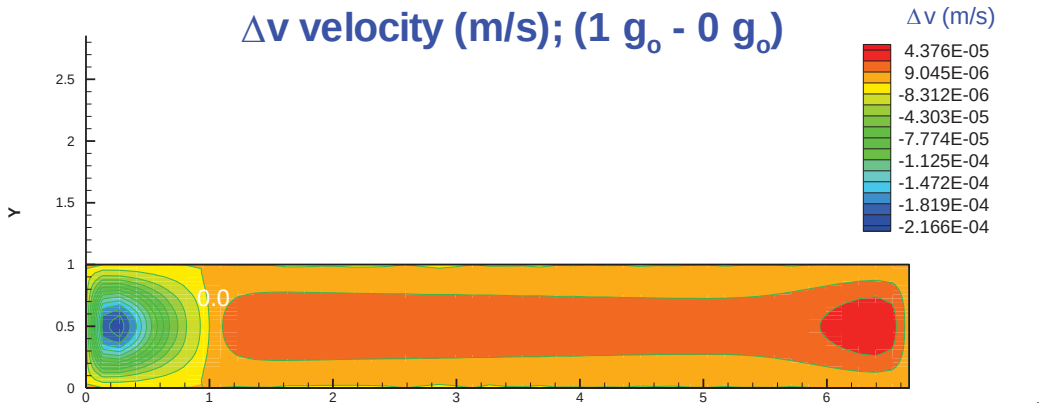

- g-sensitivity (horizontal case) based on max. buoyancy driven flow normal to growth direction is 10% of crystal growth rate (3mm/day or 0.035 μm/s)

transverse acceleration requirement: ~ 1x10^{-4} g$_o$

Gravity Effect on Velocity Difference (vertical case)

- g-effects with crystal temperature variation, Tc = Tc(y).
  Stabilized orientation: $\Delta U \sim 23.1\ \mu m/s$; $\Delta V \sim 9.4\ \mu m/s$

- g-effects with crystal temperature variation, Tc = Tc(y).
  Destabilized orientation: $\Delta U \sim 18.1 \mu m/s$; $\Delta V \sim 9.4\ \mu m/s$

As far as transverse velocity difference is concerned both vertically stabilized and destabilized orientations have similar effects

- g-sensitivity (vertical case) based on max. buoyancy driven flow normal to growth direction is 10% of crystal growth rate (3mm/day or 0.035 μm/s)

longitudinal acceleration requirement: ~ $2.7 \times 10^{-3}\ g_o$

ZnSe with Residual Gas - 3D Calculation Results

- significant flow observed along the ampoule axis (z-direction) indicative of more deposition in the central area than near the walls
- velocity contours in the cross planes(x-y) show appreciable variation only near the end walls (source and crystal)
- species (Zn and Se_2) show fairly uniform distributions in the cross planes
- predicted crystal growth rate from 2-D and 3-D calculations are in fair agreement

Summary of Theoretical Calculation

- 2D and 3D calculations performed for ZnSe system
- Residual gas effects considered
- Calculations show that shear flow velocities of 10 to 50 microns/s are induced by buoyancy effects (290 to 1400 times growth rate)
- g-level requirements established based on time scale analysis
  required transverse g level: $< 1.2 \times 10^{-4} g_o$
  required longitudinal g level $< 8.5 \times 10^{-3} g_o$
- It is noted that the Boussinesq model used in the calculations tend to underpredict velocities

Flight Experiments on International Space Station

- The flight experiments will be conducted in the Low Gradient Furnace (LGF) in the Microgravity Science Research Rack (MSRR) on International Space Station (ISS)

- Nine different growth runs will be performed for ZnSe, Cr-doped ZnSe, ZnSeTe, ZnSeS and ZnCdSe materials with different growth parameters.

- The flight experiments are scheduled to commence in late 2015.

Refereed Publications on Vapor Growth

"Growth Rate of CdS by Vapor Transport in a Closed Ampoule." J. Crystal Growth, 80 333-342 (1987).

"Growth and Characterization of CdS Crystals". J. Crystal Growth, 101 221-225 (1990).

"Vibronic Spectra of Cu^{+2} in ZnTe". Phys. Rev. B, 46 76-82 (1992).

"Growth of ZnTe by Physical Vapor Transport and Traveling Heater Method". J. Crystal Growth, 128 627-632 (1993).

"Thermodynamic Analysis and Mass Flux of the HgZnTe-HgI_2 Chemical Vapor Transport System". J. Crystal Growth, 131 574-588 (1993).

"Characterization of Growth Defects in ZnTe Single Crystals". Mater. Res. Soc. Symp. Proc., Infrared Detectors - Materials, Processing, and Devices, A. Applebaum and L. R. Dawson (eds.) 299 203-208 (1994).

"Photoluminescence of Vapor and Solution Grown ZnTe Single Crystals". J. Crystal Growth, 138 219-224 (1994).

"Synchrotron Topography Characterization of ZnTe Single Crystals". Mater. Sci. & Eng. B27, 143 -153 (1994).

"Mass Flux of ZnSe by Physical Vapor Transport". J. Crystal Growth, 146 42-48 (1995).

Refereed Publications on Vapor Growth

"CdTe I: Solidus Curve and Composition-Temperature-Tellurium Partial Pressure Data for Te-Rich CdTe(s) from Optical Density Measurements". J. Phys. Chem. Solids 57 443-450 (1995).

"CdTe II: Defect Chemistry". J. Phys. Chem. Solids 57 451-460 (1995).

"Selenium Precipitation in ZnSe Crystal Grown by Physical Vapor Transport". J. Crystal Growth 147 292-296 (1995).

"Post-growth Annealing of CdS Crystal Grown by Physical Vapor Transport". J. Crystal Growth 166 721-735 (1996).

"Partial Pressures of Zn and Se_2 over ZnSe(s) from Optical Density Measurements". High Temp. and Mater. Sci. 35 215-237 (1996).

"Mass Flux and Partial Pressures of ZnSe by Physical Vapor Transport". J. Crystal Growth 166 736-744 (1996).

"Analysis of the Zn-Se System". J. Phase Equilibria 17 495-501 (1996).

"Mass Flux of $ZnSe_{1-x}S_x$ and $ZnSe_{1-x}Te_x$ by Physical Vapor Transport". J. Crystal Growth 171 516-524 (1997).

"Vapor Phase Stoichiometry and Heat Treatment of CdTe Starting Material for Physical Vapor Transport". J. Crystal Growth 183 519-524 (1998).

Refereed Publications on Vapor Growth

"Segregation Coefficients of Impurities in Selenium by Zone Refining". J. Crystal Growth 187 569-572 (1998).

"Characterization of Semi-insulating CdTe Crystals Grown by Horizontal Seeded Physical Vapor Transport", J. Crystal growth 191 377-386 (1998).

"Heat Treatment of ZnSe Starting Materials for Physical Vapor Transport", To be published on J. Crystal Growth. Ching-Hua Su, W. Palosz, S. Feth and S. L. Lehoczky, "Heat Treatment of ZnSe Starting Materials for Physical Vapor Transport", J. Crystal Growth. 192 386-394 (1998).

"Point Defect Distributions in ZnSe Crystals: Effects of Gravity Vector Orientation during Physical Vapor Transport", J. Crystal Growth 204 41-51 (1999).

"Vapor Growth and Characterization of Cr-doped ZnSe Crystals", J. Crystal Growth 207 35-42 (1999).

"Characterization of ZnSe Single Crystals Grown by Physical Vapor Transport", J. Crystal Growth 208 237-247 (2000).

"Modeling Studies of PVT Growth of ZnSe: Current Status and Future Course", J. Crystal Growth 208 269-281 (2000).

"In-situ Partial Pressure Measurements and Visual Observation during Crystal Growth of ZnSe by Seeded Physical Vapor Transport", J. Crystal Growth 209 687-694 (2000).

Refereed Publications on Vapor Growth

"Contactless Growth of ZnSe Single Crystals by Physical Vapor Transport", J. Crystal Growth 213 267-275 (2000).

"Vapor Growth and Characterization of ZnSeTe Solid Solutions", J. Crystal Growth 216 104-112 (2000).

"Optical Characterization of Bulk ZnSeTe Solid Solutions", J. Appl. Phys. 88 5148-5152 (2000).

"Photoluminescence Studies of ZnSe Starting Materials and Vapor Grown Bulk Crystals", J. Crystal Growth 224 32-40 (2001).

"The Preparation Conditions of Chromium doped ZnSe and Their Effect on the Infrared Luminescence Properties", J. Crystal Growth 225 249-256 (2001).

"Beer Law Constants and Vapor Pressures of HgI_2 over HgI_2(s,l)", J. Crystal Growth 235 313-319 (2002).

"Band Anticrossing in Highly Mismatched Compound Semiconductor Alloys", Proceeding of the 28th International Symposium on Compound Semiconductors (ISCS2001).

"Partial Pressures of Te_2 and Thermodynamic Properties of Ga-Te system", Thermochimi. Acta. 390 21-29 (2002).

"Partial Pressures of In-Se from Optical Absorbance of the Vapor", J. Phase Equilibria 23 397-408 (2002).

Refereed Publications on Vapor Growth

"Composition Dependence of the Hydrostatic Pressure Behavior of the Bandgap of ZnSeTe Alloys", Phys. Rev. B, 68 033206(1-4) (2003).

"Origin of the Large Bandgap Bowing in Highly Mismatched Semiconductor Alloys", Phys. Rev. B, 67 035207(1-5) (2003).

"Thermal expansion coefficient of ZnSe crystal between 17 and 1080 °C by interferometry", Materials Letters, Vol. 63, 1475-1477 (2009).